

Deliverable D2.3

Manual guide for methodologies for physically simulating AM process and laser-surface interaction

Funded by the European Union. Views and opinions expressed are however those of the author(s) only and do not necessarily reflect those of the European Union. Neither the European Union nor the granting authority can be held responsible for them.

Copyright © by DILAPRO All Rights Reserved | D2.3 - Manual guide for methodologies for physically simulating AM process

Revision	Date	Author/Organisation	Description
1	28/02/25	IMDEA	Concept of the Deliverable
2	08/04/25	IMDEA	First draft
3	28/04/25	IMDEA, DTI, DCU	Revised document
4	31/07/25	IMDEA, DTI, DCU	Revised document, Part II has been added.



Action number: #101138859

Action Acronym: DILAPRO
Action Name: Digital Laser Production

Deliverable Due date: 30/04/25
Deliverable hand-in date: 31/07/2025

Copyright © by DILAPRO All Rights Reserved | D2.3 - Manual guide for methodologies for physically simulating AM process

Table of contents

1. List of abbreviations 3

2. Executive Summary 4

3. Part 1: Manual guide for methodology for physically simulating AM process 5

3.1 Introduction 5

3.2 Manual guide for the methodology for physical simulation of additive manufacturing process 7

3.3 Physical simulation experiment 9

3.4 Analysis of samples after physical simulation experiment 12

3.5 Conclusions to Part 1 16

4. Part 2: Review report on modelling approaches for Laser Surface Texturing using ultrafast lasers 17

4.1 Introduction 17

4.2 Modelling Tools for Laser Texturing Process 25

4.3 Machine Learning based modelling 35

4.4 Supervised and Unsupervised Learning 36

4.5 Conclusion to Part 2 41

Bibliography 42

Copyright © by DILAPRO All Rights Reserved

1. List of abbreviations

AI	Artificial Intelligence
AM	Additive Manufacturing
ANN	Artificial Neural Network
CAD	Computer Assisted Design
CCD	Charge-Coupled Device
CFD	Computational Fluid Dynamics
CW	Continuous Wave
DBSCAN	Density-Based Spatial Clustering of Applications with Noise
DED	Direct Energy Deposition
DOE	Duffractive Optical Elements
DT	Decision Trees
EBSD	Electron Backscatter Diffraction
EDS	Energy Dispersive Spectroscopy
FEA	Final Element Analysis
FEM	Final Element Method
GAN	Generative Adversarial Network
GP	Gaussian Process
HAZ	Heat Affected Zone
IN	Inconel
IR	Infrared (camera)
KNN	K-Nearest Neighbours
LMD	Laser Metal Deposition
LIPSS	Laser-Induced Surface Structures
LPBF	Laser Powder Bed Fusion
LST	Laser Surface Texturing
MD	Molecular Dynamics
ML	Machine Learning
MSDAE	Multiscale Convolutional Denoising Auto-Encoder
OM	Optical Microscopy
PCA	Principal Component Analysis
PDE	Partial Differential Equation
RF	Random Forest
RSM	Response Surface Modelling
SEM	Scanning Electron Microscopy
SS	Stainless Steel
SVM	Support Vector Machines

Copyright © by DILAPRO All Rights Reserved

TEM	Transmission Electron Microscopy
TTM	Two-Temperature Models
WAAM	Wire Arc Additive Manufacturing
WP	Work Package

2. Executive Summary

This deliverable consists of two parts. The first part presents a manual for the physical simulation of the additive manufacturing process developed within the framework of Task 2.1 under Work Package 2: *Optimization and modeling of laser technologies*. It explains the importance of physically simulating additive manufacturing and highlights the benefits of its application. The document provides a detailed description of the required sample geometry, sample preparation, and experimental setup. Additionally, it outlines the experimental procedure and the subsequent analysis of the samples after the physical simulation. The developed tool enables experimental analysis of the evolution of microstructure and properties at various stages of the additive manufacturing process (e.g., rapid solidification and thermal cycling due to subsequent layers).

Initially, the DILAPRO project planned to develop a physical simulation tool also for laser – surface interaction during Laser Surface Texturing (LST) as well. However, it was later realized that this is currently not feasible due to two factors: (1) the lack of experimental capabilities to measure thermal profiles in the subsurface during LST, and (2) the formation of highly graded microstructures in the subsurface area following laser surface texturing. The data that would otherwise be collected from the physical simulation experiments had to be collected otherwise. Therefore, a thorough literature review of existing simulation tools and modelling approaches was conducted, which can be found in the second half of the present deliverable. It is a review of LST process using ultrafast lasers and outlines a pathway to understanding the simulation tools and modelling approaches employed in this field. The objective of the review report is to focus on Task 2.3 under WP2: *Simulations of the laser material Interactions*. With an emphasis on surface modifications, this review attempts to compile the modelling tools and techniques currently employed to characterize femtosecond laser-material interactions. The report will form the basis for future modelling development work within DILAPRO and will feed into WP7 focusing on integrating the modelling tools into the DILAFACT and DILACERT solutions.

This document is a re-submission, previously approved by the project officer, following a partial change in scope. It replaces the originally planned physical simulation of laser–surface interaction with a detailed review of LST modelling, reflecting the updated and agreed project direction.

Copyright © by DILAPRO All Rights Reserved

3. Part 1: Manual guide for methodology for physically simulating AM process

3.1 Introduction

Physical simulation of materials processing involves the exact reproduction of the thermal and mechanical processes in the laboratory that the material undergoes during actual fabrication or end-use [1]. A small sample of the actual material is used in the simulation, following the same thermal and mechanical profile that it would experience in full-scale fabrication or end-use scenarios. This is achieved using specially designed thermo-mechanical simulators that can precisely control parameters of metallurgical processes. For example, instead of forging a meter-scale steel ingot, a small cylinder with the same geometry undergoes compression testing, following the same forging parameters (temperature, heating and cooling rates, deformation mode, strain, strain rate, etc.) (Figure 1). The microstructure and properties of the tested small samples are then analyzed, and the optimum processing parameters needed to achieve the desired microstructure and properties are determined.

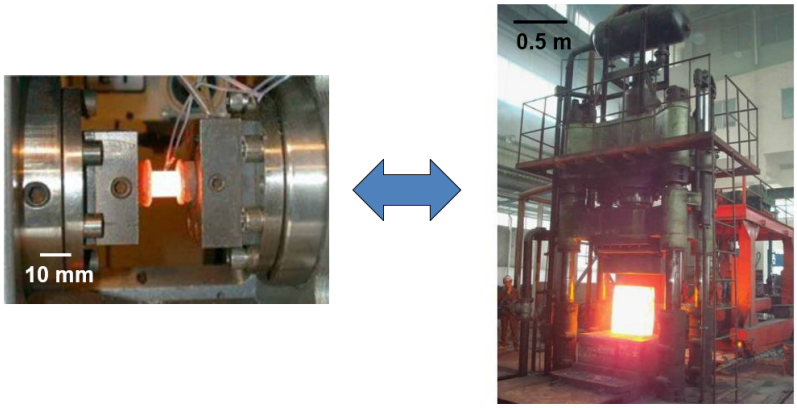


Figure 1. Reproducing forging by high strain rate compression testing in GLEEBLE 3800 thermo-mechanical simulator.

When the simulation is accurate, the results can be readily transferred from the laboratory to the full-scale production process, thus avoiding the large-scale trial-and-error approach, material waste, and labor intensity, while significantly reducing costs. **It is important to note that physical simulation is not the same as mechanical testing following certain standards, as is often perceived**. While all physical simulations involve some form of physical testing, the key difference is that physical simulation seeks to replicate real-world processes on a laboratory scale, ensuring that the resultant data can be used to solve real-world problems.

Copyright © by DILAPRO All Rights Reserved

Additive manufacturing is a relatively novel process compared to traditional metallurgical processes. Physical simulation methodologies were developed for processes such as rolling [2], forging [3], welding [4], extrusion [5], casting [6], and other conventional methods. Using these methodologies in a research lab, one can effectively determine optimum processing parameters and study the evolution of microstructure and properties during the manufacturing process. However, to date, no tool has been developed for the physical simulation of the additive manufacturing process. Such tools could offer substantial benefits to the additive manufacturing community, as outlined below.

Physical simulation could allow us to study the evolution of the microstructure during the additive manufacturing process. **The microstructure developed in an additively manufactured part results from rapid solidification after melting, followed by numerous thermal cycles as further material is deposited on top**. In traditional additive manufacturing, only the final microstructure can be studied. However, with physical simulation, we can stop the testing at any stage (right after rapid solidification, after the first thermal cycle, the second, etc.) and perform thorough microstructural characterization (e.g., phase composition, phase morphology, chemical segregation, etc.). This approach would enable a deeper understanding of the metallurgy of the additive manufacturing process and provide high-quality data to support the development of digital twins.

Physical simulation could help improve the quality of additively manufactured products. For example, it could help identify the stage at which (micro)cracking occurs and the underlying reasons for cracking, such as segregation of alloying elements or the presence of undesired second phases. This would allow necessary modifications to the chemistry of the printed alloy to prevent (micro)cracking.

A better understanding of the metallurgy of the additive manufacturing process and its sensitivity to chemical composition can help avoid wasting expensive feedstock and valuable machine time, while also reducing overall waste.

Some alloys are prone to cracking and cannot be processed effectively in additive manufacturing. Physical simulation can provide valuable insights into their compatibility with AM processes. Furthermore, a physical simulation tool could facilitate the rapid prototyping of post-processing heat treatment parameters, optimizing the final properties of the additively manufactured parts. **This document provides a manual for the methodology of physical simulation of the additive manufacturing process being developed within the framework of the DILAPRO project.**

Copyright © by DILAPRO All Rights Reserved

3.2 Manual guide for the methodology for physical simulation of additive manufacturing process

3.2.1 Preparation of sample for physical simulation

This methodology is developed for GLEEBLE thermo-mechanical simulators. It is one of the unique advantages the Gleeble system has over any other testing machines that the Gleeble system is able to conduct melting and solidification studies. Figure 2 illustrates a geometry of samples recommended for physical simulation, and its appearance is shown in Fig. 3a. A testing specimen with a diameter of 10 mm and a length of 121.5 mm is used. The non-threaded portion of the specimen is about 90 mm. For this geometry, a quartz tube with a slot on top is often used (Fig. 3b). The inside diameter of the quartz tube must be chosen properly to control melting smoothly. Normally, a 10.2 mm inside diameter quartz tube is suitable for 10 mm diameter specimen to hold the liquid metal in the mid span. Either two large or too small would induce difficulties during melting. When the inside diameter is too large, the molten metal sinks, and the specimen would be out of shape along the specimen axis. During sinking, the thermocouple tends to be detached which results in a failure of temperature control. If the inside diameter is too small, the tube will break when the specimen is expanding. With the right size of the quartz tube, it is easy to control the melting and solidification process. Core to surface thermal gradients can be substantially reduced during solidification by insulating the quartz tube, for example, using a graphite foil (Fig. 3c). It will also prevent the quartz tube from failure if it cracks during the experiment.

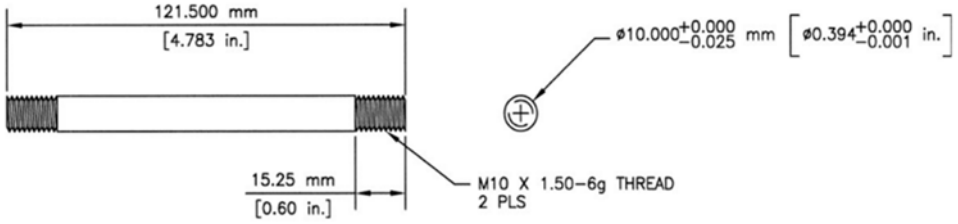


Figure 2. Geometry of samples for physical simulation.

A controlling thermocouple is welded onto the midsection of the sample (Fig. 3d). The maximum allowable temperature must be carefully considered when selecting a suitable thermocouple. For steels, titanium alloys, and nickel-based superalloys, R-type thermocouples are recommended, whereas J-type thermocouples are more suitable for aluminum alloys.

Copyright © by DILAPRO All Rights Reserved | D2.3 - Manual guide for methodologies for physically simulating AM process

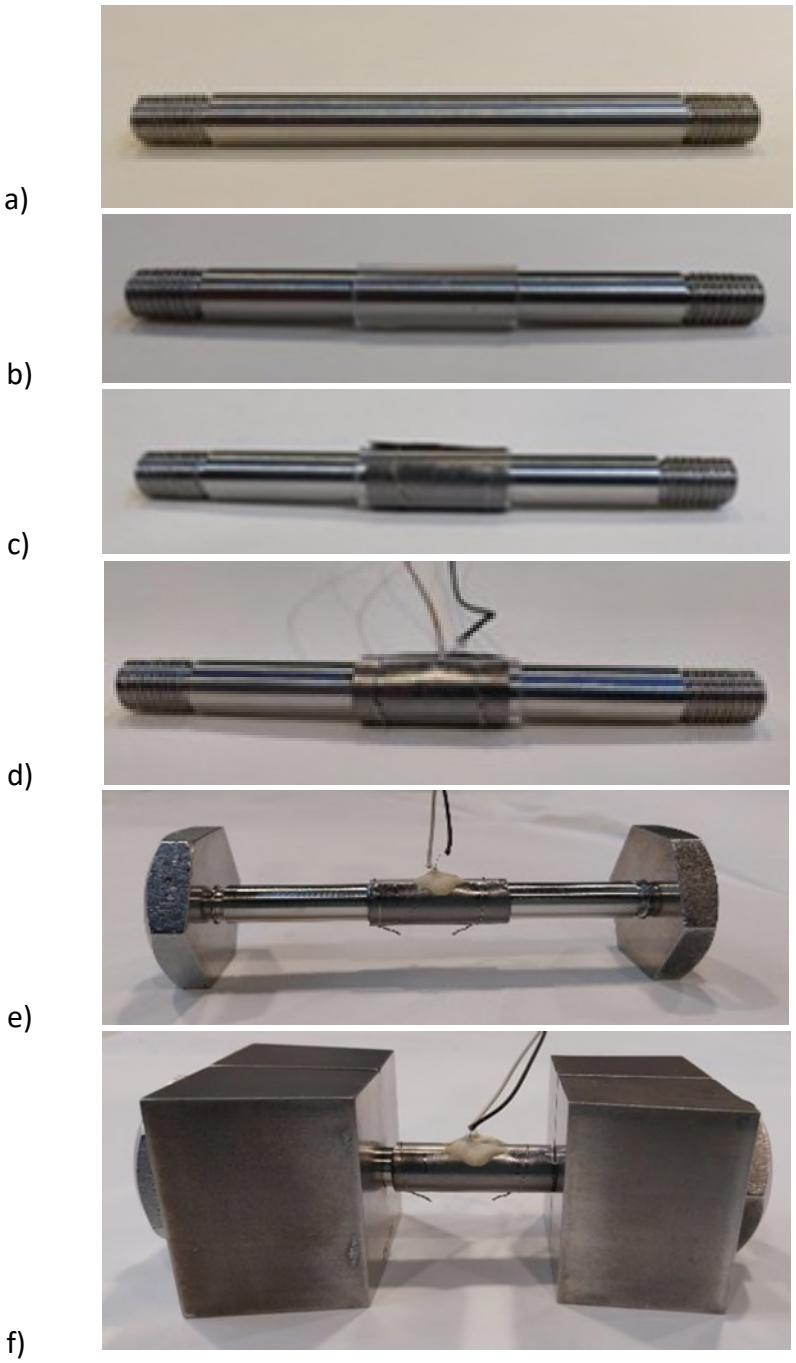


Figure 3. Sample preparation steps for physical simulation using GLEEBLE system.

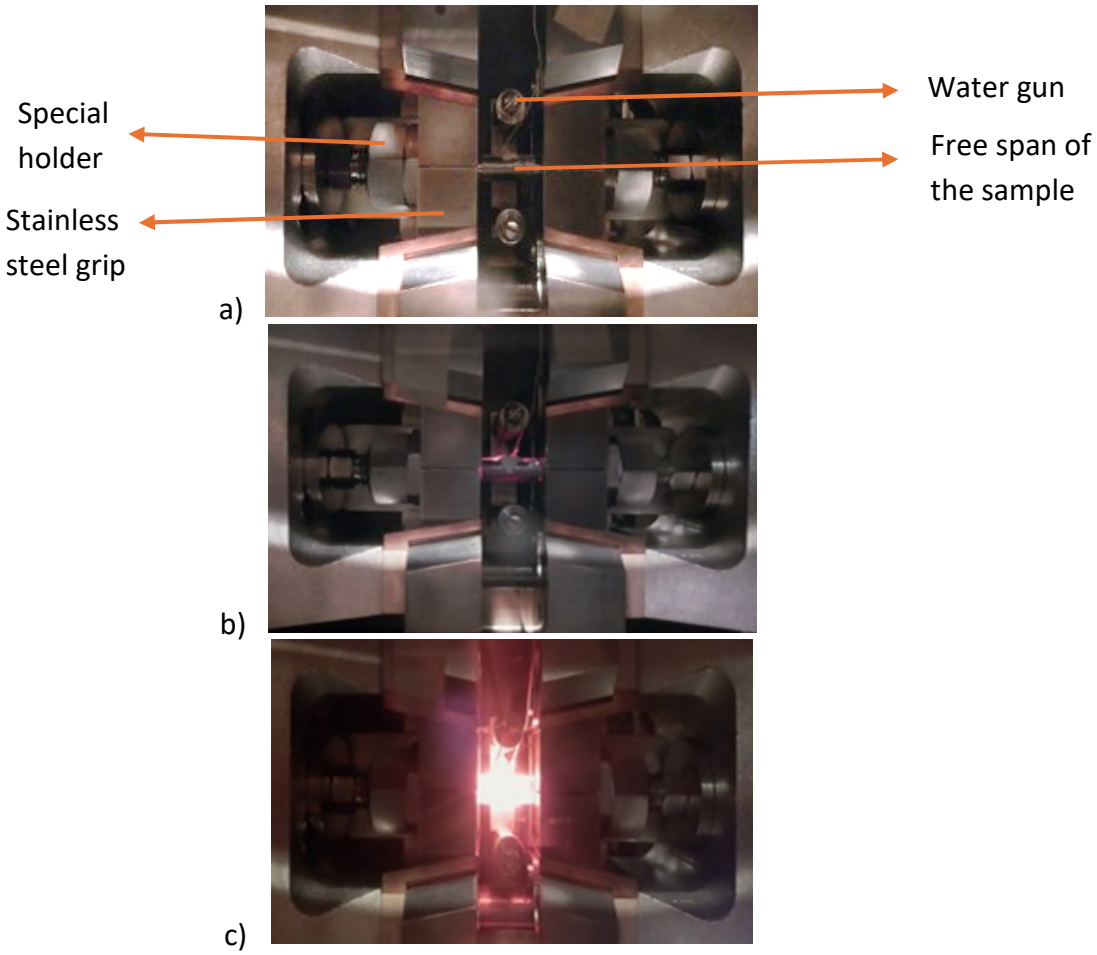
One of the challenges is securing the thermocouple during melting, as it cannot be supported directly once the specimen is in a molten state. A common solution is to use Omega Bond 400, a water-soluble cement. The cement is mixed with water and applied at the junction of the thermocouple to hold the wires against the quartz tube. Then, fixing nuts can be screwed onto

the threaded section of the ready sample to prepare it for the experiment (Fig. 3e). Finally, the sample is placed in stainless steel grips (Fig. 3g).

A water gun should be fixed inside the GLEEBLE chamber before the experiment, and the water quench system should be filled with water. The water pressure should be around 35 psi. A sample with grips (Fig. 3f) is placed into jaws inside GLEEBLE chamber and secured by special holders (Fig. 4a).

3.3 Physical simulation experiment

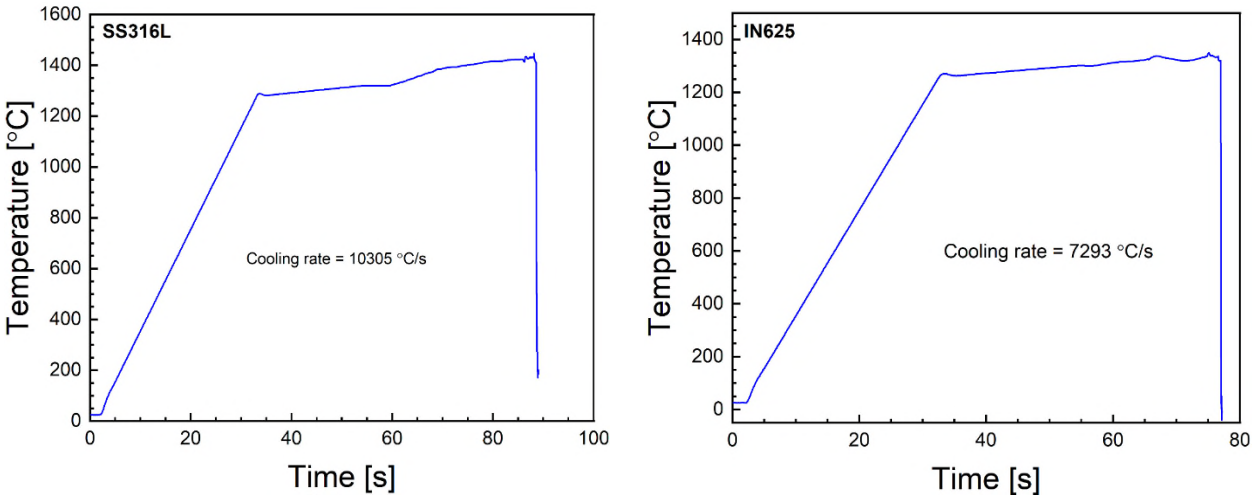
The additive manufacturing process consists of rapid solidification of molten metal followed by its thermal cycling. Therefore, the first step is to perform physical simulation of rapid solidification. The sample is heated quickly with the heating rate of 20-40 °C/s to a temperature of around 100 °C below the melting point of the material (Fig. 4b). The heating rate is then reduced to 1-2 °C/s until the melting of the midsection is observed (Fig. 4c). After that, the current is cut, and pressurized water is sprayed onto the molten metal (Fig. 4d).



d) 

Figure 4. Physical simulation of rapid solidification in the GLEEBLE system.

The cooling rate recorded during such experiments is typically in the range of ~3.000-10.000 °C/s depending on the tested material, water pressure and quality of the sample preparation. Figure 5 below presents examples of temperature- time plots from the rapid solidification experiments on SS 316L (Fig. 5a) and IN625 (Fig. 5b). These cooling rates are relevant to those observed during DED and WAAM processes [7, 8]. For instance, cooling rates between 1000 °C/s and above 5000 °C /s were experimentally measured for IN718 in [8] depending on the AM process parameters.



a) b)

Figure 5. Temperature – time plots from physical simulation of rapid solidification in GLEEBLE 3800 system: a) for SS 316 L; b) for IN625.

Much higher cooling rates of ≥ 15.000 °C/s were measured during LPBF process, although this cooling rate can drop down to ~ 5.000 °C/s when the base plate is additionally pre-heated [9]. The latter cooling rate during LPBF can also be reproduced in these GLEEBLE experiments.

The second step is to apply thermal cycling seen by the rapidly solidified zone during deposition of the upper layers. The rapidly solidified zone acts like heat affected zone (HAZ) in multi-pass

Copyright © by DILAPRO All Rights Reserved

welding processes. These thermal cycles can be either obtained via modelling [10] or experimentally measured using online monitoring tools (e.g. IR cameras or thermocouples integrated into additive manufacturing machines). The GLEEBLE system can control heating rates up to several thousand degrees per second in a solid metal which is relevant to those measured when the local temperature of rapidly solidified zone is affected by deposition of next layers (Fig. 6b). Any number of thermal cycles can be applied simulating deposition of different numbers of layers.

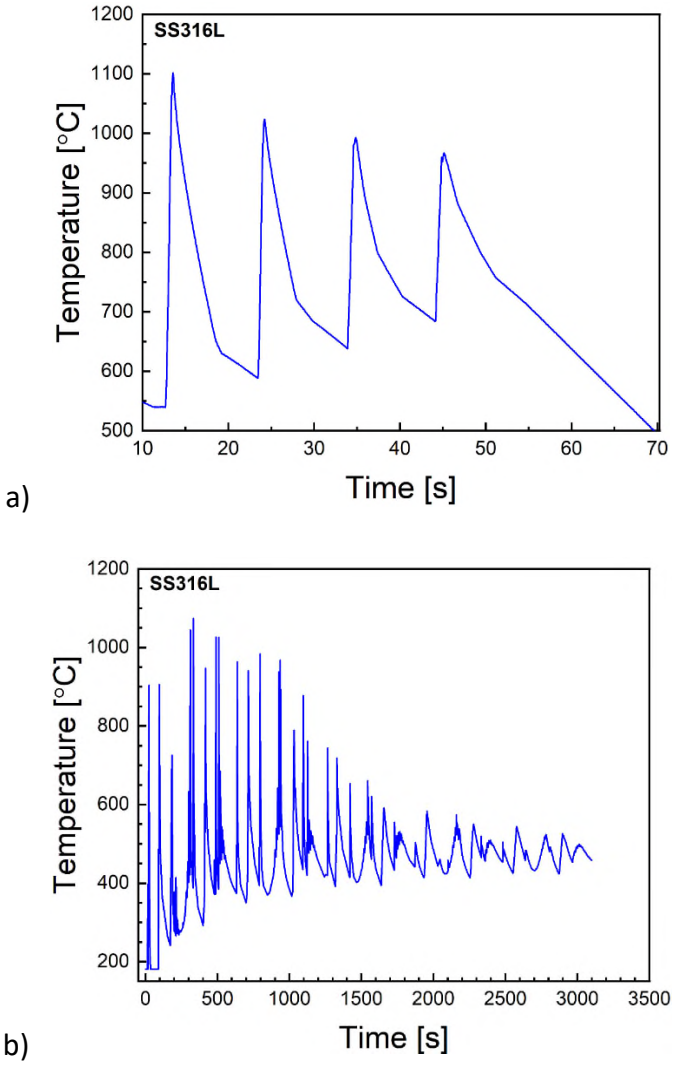


Figure 6. Temperature – time plots corresponding to thermal cycles seen by rapidly solidified area during additive manufacturing process: a) theoretically modelled for SS 316L [10]; b) experimentally measured by CRM Liege during DED of SS 316L using HYMAX system.

Copyright © by DILAPRO All Rights Reserved | D2.3 - Manual guide for methodologies for physically simulating AM process

3.4 Analysis of samples after physical simulation experiment

Figure 7 demonstrates appearance of a sample after physical simulation of rapid solidification followed by thermal cycling in GLEEBLE 3800 system. This sample can be cross sectioned for further characterization. It is recommended to focus analysis on the region below the controlling thermocouple, as the local temperature profiles of other regions may be affected by temperature gradients unavoidably present in samples during physical simulation experiments.



Figure 7. Appearance of a sample after physical simulation of rapid solidification.

The microstructural characterization can include but is not limited to optical microscopy (OM) analysis, scanning electron microscopy (SEM) analysis, electron backscatter diffraction (EBSD) analysis, energy dispersive spectroscopy (EDS) analysis, and transmission electron microscopy (TEM) analysis. Phase composition, homogeneity of distribution of alloying elements in the microstructure, dislocation density, spatial distribution of secondary phases, possible presence of (micro)cracks and the reasons for their formation can be analyzed. A few examples of such analysis are presented below.

Example 1. Microstructure formed immediately after rapid solidification

Figure 8 presents microstructure of SS 316L after physical simulation of rapid solidification in the GLEEBLE 3800 system. Predominantly cellular structure is observed (Fig. 8a). EDS analysis has revealed microsegregations of Nb (Fig. 8c) and Cr (Fig. 8d) and depletion of Fe (Fig. 8f) along cell boundaries.

Copyright © by DILAPRO All Rights Reserved

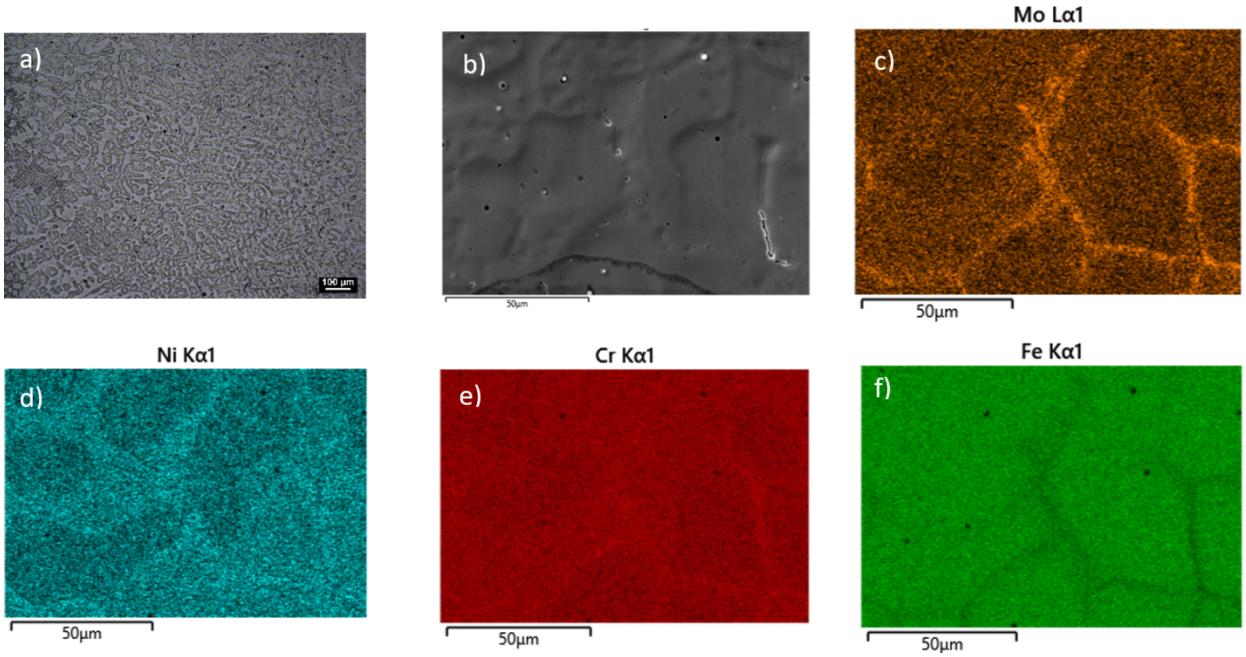


Figure 8. Microstructure of SS 316L after physical simulation of rapid solidification: a) SEM image; b) band contrast map; c-f) corresponding EDS elemental maps.

Table 1. Local chemical compositions (wt. %) in the rapidly solidified SS 316L before and after thermal cycling experiments (Fig. 8, Fig. 9).

Elements	**After rapid solidification in GLEEBLE (first step)**		**After rapid solidification in GLEEBLE (first step) followed by thermal cycling (second step)**	
	Segregated / depleted region	Non-segregated region	Segregated / depleted region	Non-segregated region
Mo	4.71	1.95	1.44	2.09
Ni	12.08	11.18	11.19	11.89
Cr	20.31	17.79	17.21	16.89
Fe	60.38	67.13	68.76	67.82

Figure 9 presents the outcomes of the EBSD analysis of the IN625 after physical simulation of rapid solidification. A cellular microstructure is observed which is in good accordance with the literature [11]. The formation of Ni_3Nb δ-phase (in blue color) along cell and grain boundaries in the γ-matrix (red color) is observed. Its volume fraction is 1.04 %. EDS analysis revealed microsegregations of Mo and Nb along grain and cell boundaries and depletion of Fe, Co and Ni. As is well known, this phase is detrimental for mechanical performance of IN625. Further thermal

Copyright © by DILAPRO All Rights Reserved

cycling will allow to study the evolution of microsegregations and local phase composition in the material, as well as provide insights into required thermal treatments after additive manufacturing process.

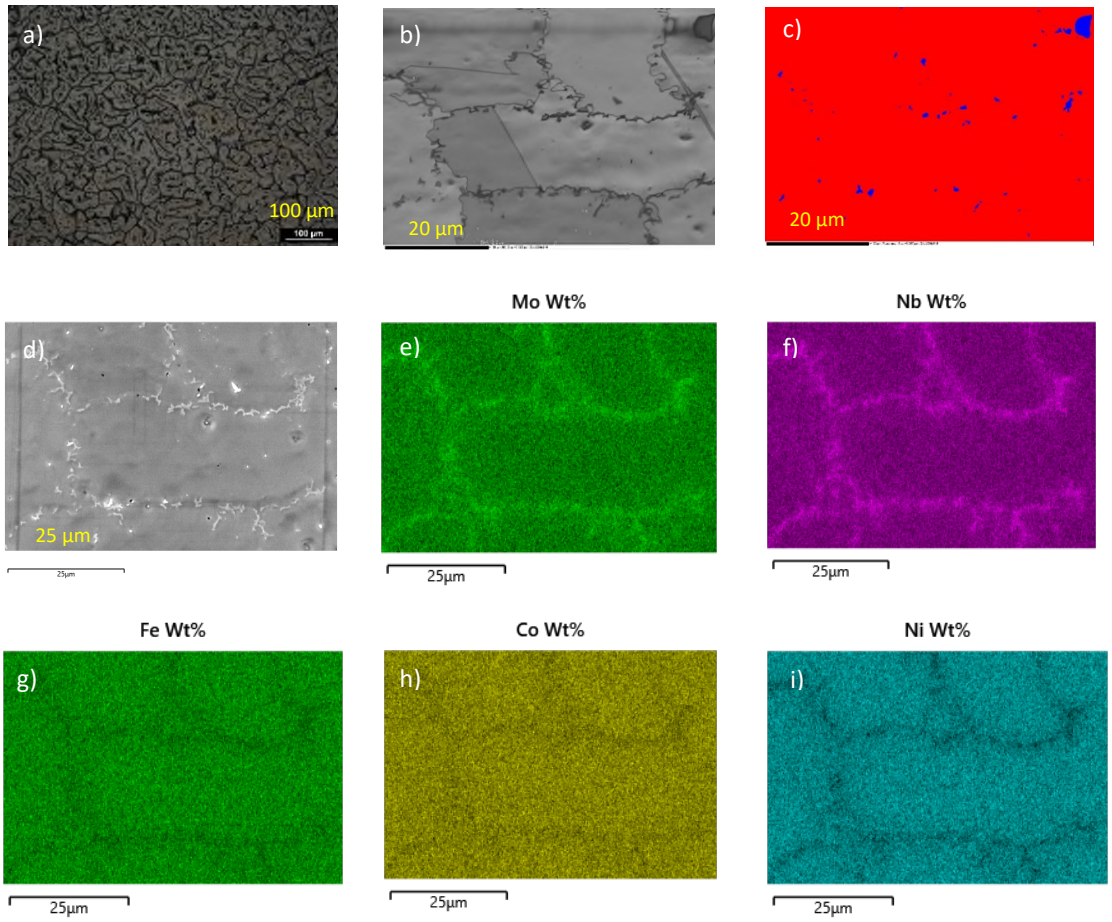


Figure 9. Microstructure of IN625 after physical simulation of rapid solidification: a) SEM image illustrating cellular microstructure; b) EBSD band contrast (BC) map; c) EBSD phase map (red – γ-matrix, blue - Ni_3Nb δ-phase); d) SEM image, e-f) corresponding EDS elemental maps.

Example 2. Microstructure evolution during deposition of further layers

The thermal cycling (Fig. 6a) simulating deposition of further layers, which is applied to rapidly solidified SS 316L sample, shows homogenization of the elemental distribution (e.g. noticeable dissolution of microsegregations on cell boundaries) (Fig. 10). Quantitative analysis of the EDS maps (Table 1) revealed that the average concentration of Mo in microsegregations is reduced from 4.71 wt. % to 1.44 wt. % and Cr from 20.31 wt. % to 17.21 wt. %, whereas the Fe content at the depleted cell boundaries is increased from 60.38 wt. % to 68.76 wt. %. It should be noted

Copyright © by DILAPRO All Rights Reserved | D2.3 - Manual guide for methodologies for physically simulating AM process

that such microsegregations have been widely reported for the additively manufactured SS 316L [12].

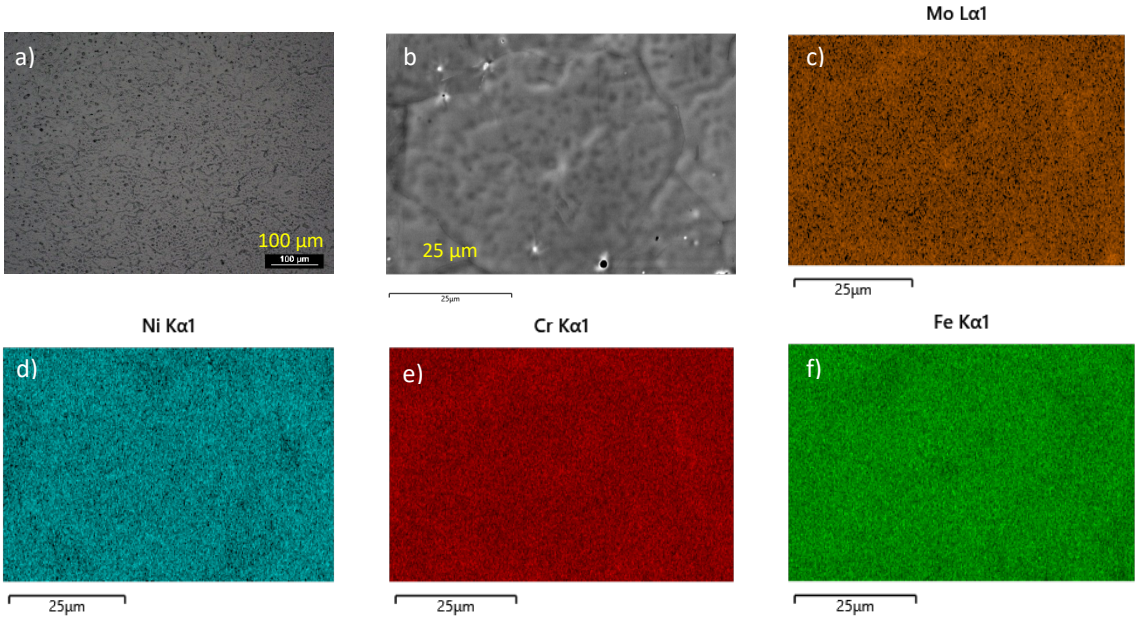


Figure 10. Microstructure of SS 316L after physical simulation of rapid solidification followed by thermal cycling (Fig. 5a): a) SEM image; b) band contrast map; c-f) corresponding EDS elemental maps.

Example 3. Analysis of mechanical properties on micro-scale

The physical simulation tool developed in the project also enables us to investigate the evolution of local mechanical properties during the AM process, which is crucial for understanding the performance of AM parts and for further improving it through microstructural (e.g., process) design. This is done by combining the microstructural characterization (SEM with EBSD and/or EDS) and mechanical characterization on micro- or nanoscale (nanohardness mapping). Figure 11 below clearly illustrates how the local microsegregations (for example, along cell boundaries) of Nb and Mo along cell boundaries in the rapidly solidified IN625 result in higher local strength.

Copyright © by DILAPRO All Rights Reserved

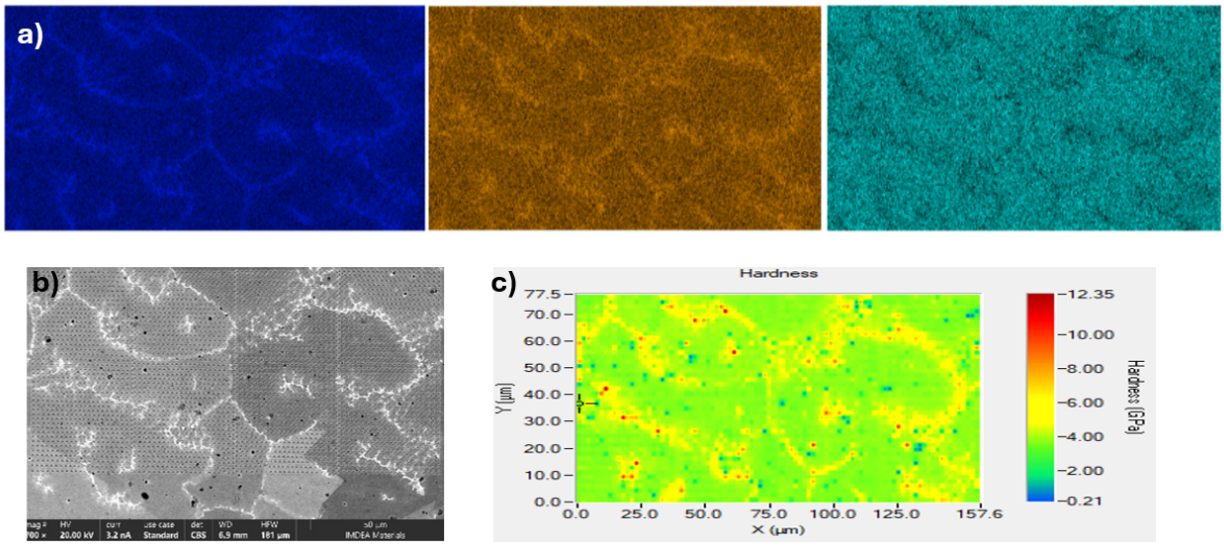


Figure 11. a) EDS maps showing local concentration of Nb, Mo, and Ni for the rapidly solidified IN625; b) corresponding surface after nanohardness mapping; c) corresponding nanohardness map.

3.5 Conclusions to Part 1

This part of the deliverable presents a novel and unique methodology for physical simulation of AM process based on GLEEBLE experiments. The methodology mimics a thermal cycle seen by metallic material during AM process: rapid solification followed by thermal cycling. The cooling rates up to 10.000 ^{o}C/s are achieved which are relevant to those measured on metallic materials subjected to DED process and LPBF process with pre-heated plate. The first experiments demonstrate that the tool is able to predict the phase compositions and microsegregations present in the AM processed SS 316L and IN625. Also, a partial dissolution of microsegregations during further thermal cycling is observed.

Copyright © by DILAPRO All Rights Reserved | D2.3 - Manual guide for methodologies for physically simulating AM process

4. Part 2: Review report on modelling approaches for Laser Surface Texturing using ultrafast lasers

4.1 Introduction

Laser surface texturing (LST) has emerged as a powerful technique for modifying the surface properties of materials to meet specific functional requirements such as tailored wetting behaviour, fouling resistance, and enhanced surface area. The motivation for simulating the LST process lies in its potential to improve a wide range of surface characteristics, including tribological performance, hydrophobicity, and thermal conductivity. Various laser types used in LST offer distinct advantages and limitations for surface modification across different materials. Commonly employed systems include continuous wave (CW) CO_2 lasers, millisecond lasers, and nanosecond pulsed lasers. However, the advent of ultrafast laser characterised by pulse durations in the femtosecond to picosecond range has revolutionized the field by enabling unprecedented precision and minimal thermal damage. The selection of laser significantly influences the result surface properties, which in turn affects the performance of materials in the tribological properties, biomedical engineering, and other engineering applications. Through controlled laser-material interactions, LST enables precise manipulation of surface topography. Ultrafast lasers, particularly femtosecond lasers play an important role in minimizing thermal effects while achieving nanoscale resolution.

This review emphasizes recent advancements in the simulation of LST, with a particular focus on ultrafast laser systems. It evaluates both data-driven and physics-based computational models, highlighting their essential role in optimizing LST processes. These kinds of models will be key in the DILAPRO softwares (DILAFACT and DILACERT), enabling prediction of surface properties and intelligent selection of processing parameters. In the coming sections, we will discuss the background and motivation for key aspects of using different lasers for the laser texturing process in engineering applications.

4.1.1 Background and Motivation

Traditional LST methods (e.g., millisecond and nanosecond lasers) rely on thermal ablation, often causing melting and recast layers near the laser processed zone. Ultrafast lasers, particularly femtosecond lasers, have revolutionized the way materials are processed at micro- and nanoscales. These lasers, characterized by their ultrashort pulse durations (10^{-15} s) and high peak

Copyright © by DILAPRO All Rights Reserved

powers, interact with materials in ways that minimize thermal diffusion and maximize precision. Over the past few decades, the demand for miniaturized, high-performance components across biomedical, aerospace, tribological, and electronics industries has spurred intensive research into femtosecond laser-material interactions. One of the most intriguing aspects of femtosecond laser processing is its complex interplay of physical phenomena, ranging from nonlinear absorption and Coulomb explosion to rapid plasma generation and phase transitions occurring under extreme nonequilibrium conditions. While this opens up remarkable possibilities for precise surface functionalization, it also introduces significant challenges in understanding and predicting surface outcomes based on laser parameters and material characteristics. As the demand for optimized surface properties such as reduced friction, improved hydrophobicity, or enhanced biocompatibility continues to grow, the need for accurate, predictive models to describe and control femtosecond laser processing has become more necessary.

Ultrafast laser texturing involves several key process parameters, including laser pulse duration, laser fluence, repetition rate, and scanning speed. These include pulse duration, laser fluence, the repetition rate, and the scanning speed. Laser fluence is the amount of energy delivered per unit area of the target material, which determines the extent of material removal and the formation of a specific microstructure on the processed surface. The optimal laser fluence depends on the physical and chemical properties of the target material. Repetition rate and scanning speed are key factors in laser processing. High repetition rates increase processing speed but increase heat accumulation and thermal damage. Slow scanning speeds improve precision, while higher scanning speeds increase processing speeds.

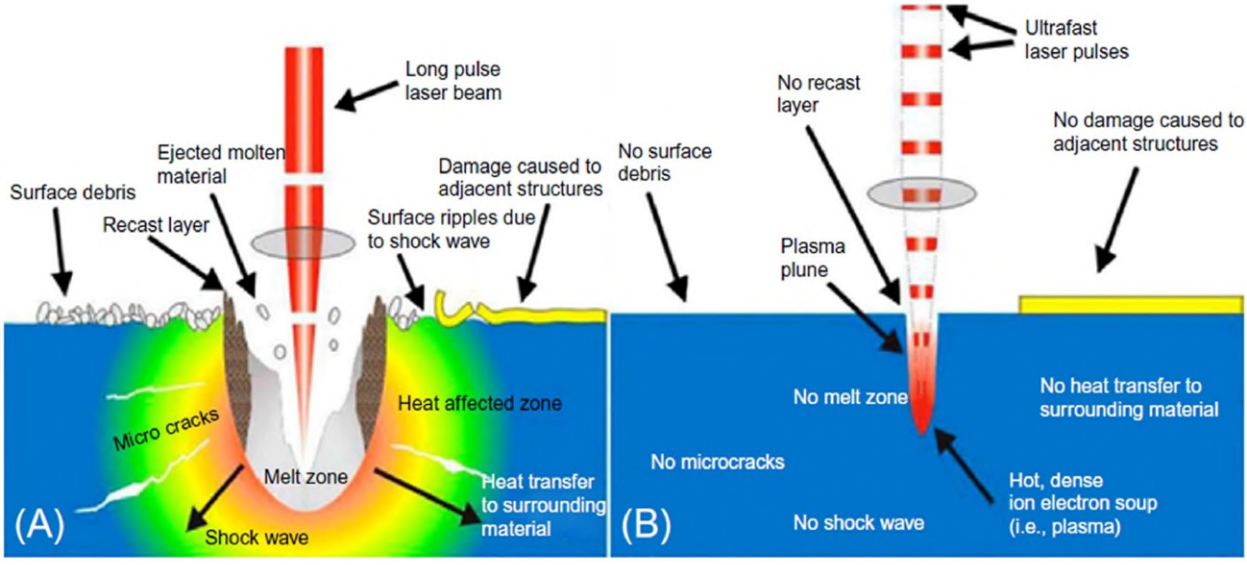


Figure 12. Schematic shows the mechanism of (a) long pulse and (b) short pulse ablation process [13].

Copyright © by DILAPRO All Rights Reserved | D2.3 - Manual guide for methodologies for physically simulating AM process

The pulse duration is an important process parameter in ultrafast laser texturing because it sets the pulse's peak power and energy density. When pulse durations are shorter, peak powers and energy densities go up, which speeds up the removal of material and makes the surface better. Femtosecond laser texturing, or cold processing, is a kind of laser that sends a short pulse of energy to the lattice before the electrons move it. Figure 12 shows the schematic illustration of the laser-ablation mechanism for both long-pulse and short-pulse processes [13].

4.1.2 Importance of Femtosecond Laser Processing in Surface Finish

Femtosecond lasers offer unparalleled advantages in surface engineering: minimal heat-affected zones, ultra-high precision, and the ability to directly write micro- and nanostructures without the need for masks or chemicals. These features make them particularly suitable for applications demanding clean, precise, and functionally enhanced surfaces. For instance, biomimetic textures created via laser-induced periodic surface structures (LIPSS) have shown potential in improving cell adhesion, reducing drag, and tailoring wettability. This characteristic fundamentally alters the laser-material interaction mechanism:

- **Minimal thermal damage**: Unlike nanosecond lasers, which cause melting and recast layers due to heat diffusion, ultrafast lasers ablate material through non-thermal processes like multiphoton absorption and Coulomb explosion. This preserves the structural integrity of the substrate [14].
- **High precision**: Due to the reduced heat-affected zone (HAZ), sub-micrometer features can be achieved [15].
- **Material versatility**: Ultrafast lasers can process advanced engineering materials including glass, transparent dielectrics, ceramics with high precision without damaging the substrastes [16–18].

These advantages make ultrafast lasers ideal for applications demanding nanoscale precision, such as medical implants or optical devices. Moreover, femtosecond laser texturing allows the generation of surfaces that mimic natural patterns, such as shark skin or lotus leaves, often in a single processing step, thereby significantly reducing manufacturing time and energy consumption.

4.1.3 Biological Inspiration and Biomimicry

Nature has long served as an inspiration for engineers and researchers in the development of surfaces with unique functional properties. Due to their nanometer- or micrometer-scale periodic features, many biological surfaces such as those found on the skin of insects, fish, and plants exhibit remarkable characteristics, including superhydrophobicity, drag reduction, and

Copyright © by DILAPRO All Rights Reserved

wear resistance [14]. These natural structures have motivated scientists to replicate such topographies artificially often termed biomimetic or nature-inspired surfaces across a variety of materials using diverse manufacturing techniques. Among these, laser surface texturing has emerged as a key tool, due to its versatility in producing intricate geometries with high precision [14]. For instance, microgrooves or nanoscale textures created on metallic implants can significantly enhance osseointegration and impart antibacterial properties. Ultrafast lasers, in particular, facilitate the fabrication of biomimetic textures on biocompatible materials, contributing to reduced surface contamination and improved functional performance due to their low thermal impact [19]. LST can create biomimetic surfaces with precise wetting properties offers numerous applications, including self-cleaning surfaces with antifouling properties, improving oil-water separation efficiency, and enhancing green energy systems like batteries and fuel cells. Figure 13 shows the application of LST to fabricate biomimetic surfaces with precise control over the fabricated surfaces.

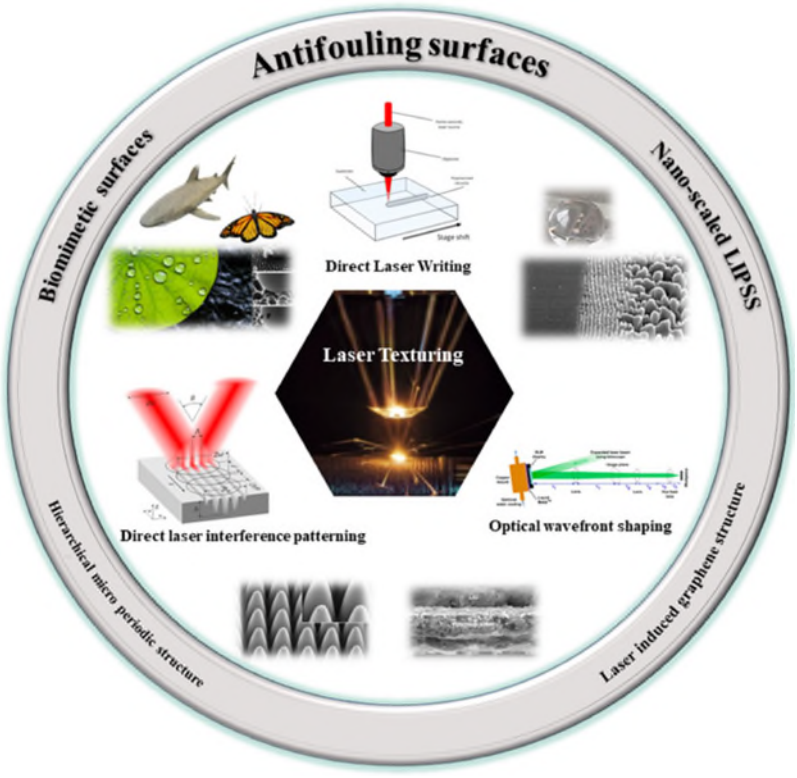


Figure 13. The diagram illustrates various laser texturing techniques utilized to create antifouling surfaces [13].

4.1.4 Application of Laser Processing in Different Sectors

Laser processing has emerged as a transformative technology across numerous industries, owing to its precision, efficiency, and versatility. Its growing adoption in sectors such as manufacturing, healthcare, aerospace and defense underscores its broad utility and impact. The following sections provide a detailed overview of laser processing applications across diverse domains:

- **Manufacturing:** Laser processing encompasses both macro-scale techniques (e.g., cutting, welding and cladding) and micro-scale techniques (e.g., micro-texturing and scribing), significantly enhancing manufacturing efficiency and product quality [20].
- **Automotive and Electronics:** Laser microprocessing plays a critical role in the fabrication of automotive components and flexible electronic devices, contributing to improved product performance and energy efficiency [21].
- **Smart Materials:** The use of laser technology enables the development of smart materials with adaptive properties, which are essential for advanced applications in healthcare, robotics, and adaptive systems [22].
- **Medical Sector:** Lasers are extensively employed in medical devices and surgical procedures, including dentistry and dermatological treatments, due to their precision, safety, and operational efficiency [23].

4.1.5 Importance of Simulation and Modelling

The simulation of the laser surface texturing (LST) process is mainly based on its ability to change the properties of surfaces to meet the needs of different fields, such as biomedical, mechanical, automotive, and marine applications. The ability to virtually design and predict surface features using computational modelling makes it possible to create textures that are specific to a certain application, which improves performance and reliability. Simulation frameworks greatly enhance the accuracy and effectiveness of LST by facilitating the optimization of process parameters and the prediction of the resulting surface characteristics. Using modelling and simulation of the textured surfaces in the DILAFACT and DILACERT software will enable intelligent selection of process parameters - based on the *specific* quality factors that are important to the specific application field. Continuing to look into the problems and limits that LST simulations face will help make them more useful, which will speed up new ideas in many fields of science and engineering.

Despite its advantages, LST faces several complexities and challenges. Computational modelling is used to predict outcomes, lower experimental costs, and hasten industrial adoption in the nonlinear dynamics of ultrafast laser-material interactions spanning plasma generation, phase transitions, and melt pool dynamics [24][25]. Advanced computational modelling and simulation are essential to understand the complexity of ultrafast laser-material interactions to maximize

processes, lower experimental costs, and hasten innovation. The important function of ultrafast lasers in texturing is investigated in this work, together with the reasons that simulations are essential for developing this technology. This section provides a comprehensive overview of the background and motivation for numerical studies of LST.

4.1.5.1. Role of Simulation in Laser Surface Texturing

Simulation plays a crucial role in the development and optimization of LST processes. The topography and characteristics of laser-textured surfaces have been predicted using computational models, such as the finite element method (FEM) and computational fluid dynamics (CFD) [24] [25]. To produce precise predictions of surface characteristics, these models take into account a number of physical phenomena, such as heat transfer, melt pool dynamics, and laser ablation [24]. The design and optimization of textured surfaces have been accelerated by the use of simulation, which has greatly decreased the need for lengthy experimental trials [25][26]. The sections below demonstrate the motivation of Multiphysics simulation for the laser texturing process.

4.1.5.1.1. Hydrophobic and Icephobic Surfaces

Laser surface texturing is a technique that improves the hydrophobic and icephobic properties of stainless steel by creating micro- and nanostructured surfaces. This process uses various laser parameters to alter wettability, allowing for tailored surface characteristics for various applications. Recent studies have shown a direct relationship between laser texturing and the hydrophobic or hydrophilic properties of metal and metal alloys such as stainless-steel alloy, Ni-based alloys, and aluminium alloy surfaces, highlighting the potential of laser surface texturing in various applications. Surfaces with custom wettability, such as icephobic and superhydrophobic surfaces have also been produced using LST. It can be used in various industrial applications, such as anti-icing, anti-slip, anti-fog, self-cleaning, biomedical applications, and energy sectors [27, 28]. The process involves various laser settings, such as nanosecond pulse lasers, which create textures that transition from superhydrophilic to superhydrophobic states. The process parameters such as scan speed, power, repetition rate and scan strategies of the laser are critical, with higher speeds and higher power settings yielding more hydrophobic surfaces, while lower settings result in hydrophilic characteristics [29]. The durability of hydrophobic and icephobic surfaces varies, with some treatments allowing for partial recovery of hydrophobic properties after chemical exposure [30]. Mechanical stability is another key factor in the durability of laser surface texturing [31]. Research indicates that hierarchical structures can enhance the long-term stability of hydrophobic surfaces against mechanical wear, maintaining their properties even under abrasive conditions.

4.1.5.1.2. Tribological Applications

Laser surface texturing (LST) is a surface engineering technique that significantly enhances the tribological performance of mechanical and automotive components by improving wear resistance and reducing friction through the generation of controlled micro- and nano-scale surface features. LST enhances lubricated contact conditions by precisely forming micro-scale features on surfaces, such as dimples or particular patterns. Zhang et al. [32] and Kumar et al. [33] have reported that these textures reduce friction coefficients and mitigate abrasive damage by efficiently trapping wear debris and encouraging the generation of advantageous hydrodynamic pressure within the contact zone. Diesel engines are a well-known example of an application where LST-generated micro-dimple textures improve lubrication regimes and thereby lower friction losses. Optimizing the surface design parameters (such as dimple density, depth, and shape) and using process simulation are essential for maximizing the efficiency and effectiveness of LST implementation. These methods not only save development time and cost but also offer a deeper thermomechanical understanding of the texturing process and its effects.

4.1.5.1.3 Thermal Applications

As LST has various applications, LST has also been used to improve thermal characteristics like heat transfer in addition to tribological and hydrophobic applications. In heat exchanger applications, for example, it has been demonstrated that laser-textured surfaces with corrugated patterns enhance heat flux [34]. Their adoption in thermal management systems has been further accelerated by the ability to design and simulate such textures using computational models [34] [26].

Table 2. Applications for Laser Surface Texturing.

Application Area	Materials	Key Findings	References
Tribological Applications	AISI 304	Laser-assisted periodic textures were fabricated to reduce the tribological behaviour of the austenitic stainless steel such as adhesion wear rate and coefficient of friction of the surface.	[35]
	AISI 52100	The study was conducted to determine the tribological performance (e.g., wear and friction resistance) of textures on the bearing steel (AISI 52100) over non-textured samples.	[36]
	SUS420J2	Laser texturing on SUS420J2 SS has been performed at different ranges of pulse duration ranges between 15 ps and 400 fs. The experimental study shows that different pulse durations significantly influence the cross-sectional profile of the wear resistance analysis.	[37]

Application Area	Materials	Key Findings	References
	IN718	Laser texturing on IN718 was performed to fabricate micro-convex dimple structures to enhance the tribological properties of the additively manufactured samples.	[38]
	IN718	Laser texturing of Inconel 718 alloy improves surface roughness, reduces friction coefficient, and enhances tribological performance by creating micro/nano-poles and pillars.	[39]
	IN718	The study explores the use of a Nd: YVO4 fibre laser for surface texturing of Inconel 718 alloys, aiming to improve properties like thermal conductivity, lightweight, and chemical resistance.	[40]
	IN718	Additively manufactured Inconel 718 alloy samples underwent laser ablation using a femtosecond laser to reduce surface roughness.	[41]
Hydrophobic and Icephobic Surfaces	IN718	Enhanced wettability and anti-icing properties through convex dimple textures.	[42]
	SS316L	The ability to tailor surface properties by fabricating features such as spikes, laser-induced periodic surface structures (LIPSS) and nanopillars. The feature helps in controlling the wettability and antibacterial properties of the surface.	[43]
	AISI 304	The study demonstrates the influence of laser power on laser surface texturing for tailoring surface wettability and improving corrosion resistance.	[44]
	AISI 304L	Ultrashort laser processing was employed on stainless steel (SS) to fabricate hierarchical surface textures aimed at enhancing wettability resistance and imparting antimicrobial properties to the SS surfaces.	[45]
	IN718	Tailored the properties of the additively manufactured parts such as wettability and roughness by surface texturing strategies.	[46]
	IN718	Laser surface texturing of Inconel 718 alloy under controlled atmospheric conditions enhances hydrophobicity and improves surface properties such as microhardness while reducing surface cracks.	[39]
Thermal Applications	SS	Direct laser selective texturing was used to improve the condensation heat transfer on stainless steel surfaces.	[35]
	SUS321	Surface texturing and molybdenizing of stainless-steel help enhance its tribological properties. This also enhances the thermal resistance of the surface.	[48]
	AISI 304L	The study illustrated the utilization of laser structuring on stainless steel to attain elevated spectral emissivity for thermal management in high-temperature systems.	[49]
	AISI 316L	The laser surface texturing was done to intensify the convective heat transfer on the surface of SS. The results show the average heat transfer coefficient increased by 16.53%.	[50]

Application Area	Materials	Key Findings	References
	IN718	The objective of laser texturing on Inconel 718 is to develop small textured areas where reinforcement materials can be added, which improves properties like thermal conductivity, which is very important for thermal applications.	[51]
	IN718	The study discusses the surface structuring of nickel-based superalloy IN718 to enhance its thermal properties with minimal material removal.	[52]
	Cr2AlC	Improved heat transfer in heat exchangers with corrugated and V-shape textures	[34]

Despite the advantages of laser surface texturing, challenges remain regarding the durability of these properties under harsh environmental conditions. Further research is needed to optimize these surfaces for practical applications [14]. It is very crucial to investigate the computational techniques that facilitate the prediction and optimization of laser-material interactions. Simulation and modelling frameworks offer a potent way to visualize process dynamics, fine-tune laser parameters, and predict the resulting surface morphologies and functional outcomes, while experimental investigations offer crucial insights. By bridging the gap between theoretical design and real-world implementation, these tools allow researchers to accurately and economically simulate a variety of laser-material scenarios. With a focus on ultrafast laser systems, the next section provides a summary of the main modelling techniques and computer systems used in the simulation of laser texturing processes. The following section discusses the available tools used for simulation and modelling for the LST.

4.2 Modelling Tools for Laser Texturing Process

In laser surface texturing (LST) process generates deterministic surface structures by precisely removing material with concentrated laser beams, frequently on micro- or nanoscale features. Due to the multi-scale and multi-physical nature of laser-matter interaction, experimental methods are often insufficient to comprehend and optimize the texturing parameters completely. Computational and Multiphysics simulations are essential for designing, managing, and forecasting surface modifications by lasers.

The simulation of laser texturing encompasses a wide array of physical phenomena, including electromagnetic wave propagation, energy absorption, heat transfer, phase transformation, material ablation, plasma generation, and thermo-mechanical stresses. Numerous software platforms and computational tools facilitate these intricate, coupled processes. These resources

comprise finite element software, commercial Multiphysics solvers, and specially developed numerical models grounded in mechanical, optical, and thermodynamic principles.

For simulating heat conduction, temperature gradients, and the resulting thermal stresses during and after laser irradiation, COMSOL Multiphysics, ANSYS, and ABAQUS are commonly utilized. Software such as Zemax OpticStudio and TracePro provide ray tracing and beam shaping features crucial for comprehending surface energy distribution when modelling optical beam propagation and focusing mechanisms. Molecular dynamics (MD) platforms, such as LAMMPS, are combined with Two-Temperature Models (TTM) to capture electron-lattice interactions at atomic scales in scenarios where non-equilibrium effects prevail, particularly when the laser pulses are ultrashort (in the femtosecond or picosecond regimes). OpenFOAM presents a versatile, open-source framework for simulating the impacts of recoil pressure and vaporization in high-fidelity fluid and plasma dynamics simulations.

Additionally, especially in cases where the experimental parameter space is extensive or data-intensive, custom-coded models are often developed using platforms such as MATLAB or Python to simulate laser scanning paths, predict ablation depth, and evolve surface patterns. These models can provide predictive control over process outcomes by integrating analytical equations, empirical relationships, and experimental calibration. Incorporating simulation tools into laser texturing workflows enables systematic process optimization, minimizes experimental trial-and-error, and accelerates the creation of functionally textured surfaces for various applications, including aerospace components and biomedical implants. Therefore, researchers and engineers engaged in laser-based surface engineering must have a thorough understanding of the software capabilities available and how to use them effectively. Depending on the degree of detail, the physical phenomena involved, and the characteristics of the material and laser, a variety of software tools can be used. A categorized list of software frequently used in laser texturing simulations can be found in Table 3.

Table 3. Simulation Tools for Laser Processing.

	Modelling Tools	**Domains**	**Applications**	**Advantages**	**Ref.**
1	COMSOL	Multi-physics FEM	Laser heating, melting, and ablation.	Versatile, highly customizable.	[53]
2	ANSYS	FEM/CFD	Heat transfer, stress modelling.	Robust mechanical simulation.	[54]
3	ABAQUS	Thermo-mechanical FEA	Thermo-mechanical analysis.	Accurate stress modelling.	[55]

4	SolidWorks	Thermo mechanical	Heat distribution, dimensional analysis.	Flexibility to complex geometries.	[34]
5	OpenFOAM	Open source CFD	Fluid/plasma flow in laser ablation.	Custom CFD, open-source flexibility.	[56]
6	Zemax OpticStudio	Optical Ray Tracing	Beam propagation and focusing.	Precision optical modelling.	[57]
7	LAMMPS	Molecular Dynamics	Ultrafast interaction at the atomic level.	Captures ultrafast non-equilibrium phenomena.	[58,59]
8	MATLAB	Custom Numerical Modelling	TTM, ablation depth, scanning paths.	Flexible for scripting and integration.	[60,61]
9	Dr. LASEM	Laser Process Modelling	Laser ablation modelling for welding/texturing.	Industry-relevant laser modelling.	[62,63]

4.2.1 COMSOL

COMSOL Multiphysics® is a simulation platform that uses finite element analysis (FEA) to model multiphysics phenomena in laser texturing and processing of metals/alloys. It integrates electromagnetic, thermal, fluid, and structural dynamics to simulate laser-material interactions, allowing for precise virtual prototyping and optimization. The platform's key functionalities include laser source modeling, multiphysics coupling, and material response. It simulates laser absorption and scattering at the surface, heat transfer, fluid dynamics, structural mechanics, and alloy-specific behavior. Applications in metal processing include texturing, optimizing cutting, welding, and additive manufacturing by analyzing heat-affected zones (HAZ), and optimizing cutting, welding, and additive manufacturing. Advantages of COMSOL include parameter optimization, predictive accuracy, and scalability. It supports 2D/3D geometries and high-performance computing for complex industrial-scale models. By integrating multiphysics dynamics, it accelerates R&D, enhances process reliability, and supports innovation in high-precision metal applications. Deshmukh et al. [64] have developed a thermal model using COMSOL multiphysics software to investigate the laser surface micro-texturing process (Figures 14, 15).

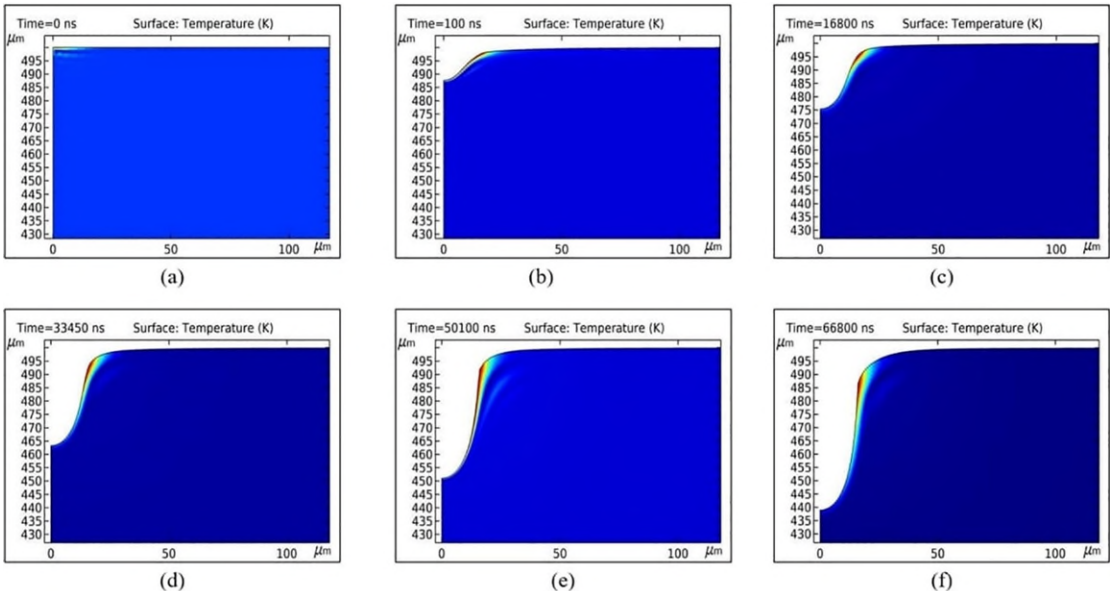


Figure 14. 2-D axisymmetric plot of deformed shape showing width and depth at different pulses. [64]

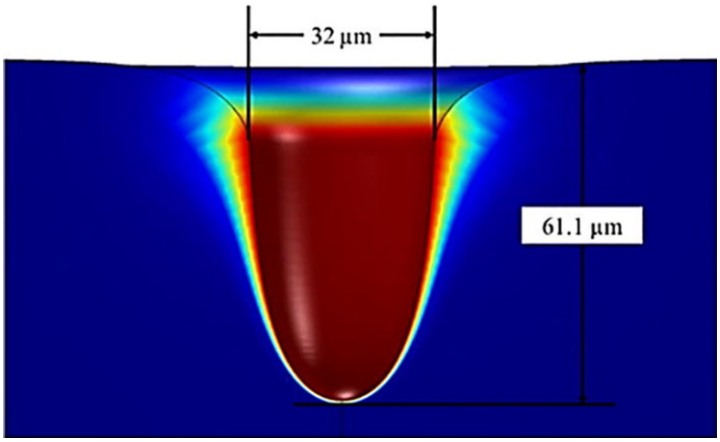


Figure 15. Predicted maximum deformation in thermal modelling using COMSOL. [64]

4.2.2 ANSYS

ANSYS simulation software is a powerful tool for modelling laser texturing and processing for metals and alloys. It uses multiphysics capabilities to make industrial workflows in an efficient manner. It eliminates the need for expensive physical experiments by forecasting results such as surface topography, microstructural alterations, and thermal stresses. In order to simulate laser-material interactions, ANSYS combines solvers for electromagnetic, thermal, and fluid dynamics. Thermal analysis, fluid dynamics, laser source modelling, and structural mechanics are important simulation mechanisms. Liu et al. [65] have used ANSYS to forecast the temperature field in the laser-irradiated area (Figure 16). By ensuring quality and repeatability in laser processes, ANSYS

Copyright © by DILAPRO All Rights Reserved | D2.3 - Manual guide for methodologies for physically simulating AM process

is used in various fields viz. aerospace, automotive, and medical devices by making sure that laser processes are consistent and of high quality. Its ability to predict accurately fits with the goals of Industry 4.0, which include real-time process monitoring and sustainable manufacturing. Overall, ANSYS provides a robust framework for simulating laser-metal interactions, driving innovation in surface engineering while minimizing resource expenditure. This leads to new ideas in surface engineering while keeping costs low.

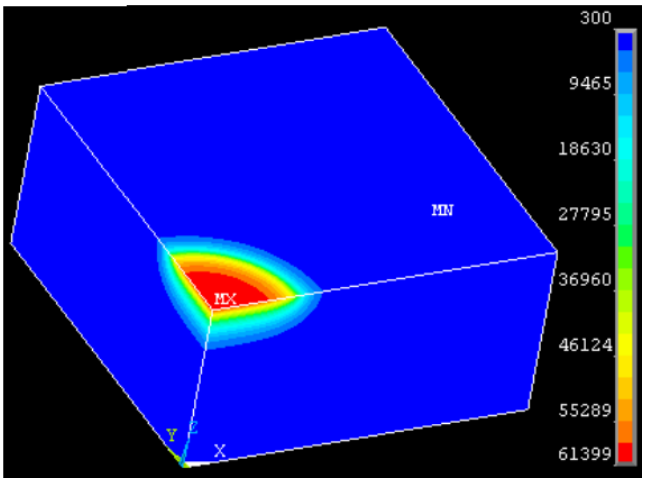


Figure 16. Temperature field of target radiated by 5-pulses. [65]

4.2.3 ABAQUS

Dassault Systemes' ABAQUS is a finite element analysis (FEA) software that enables high-fidelity simulation of laser texturing and processing for metals and alloys. It models complex thermo-mechanical interactions during laser-material interactions, aiding in optimizing parameters and predicting outcomes like surface morphology, residual stresses, and microstructural changes. ABAQUS integrates thermal and mechanical solvers to simulate laser-induced heating, melting, vaporization, and rapid solidification, accounting for temperature-dependent material properties and phase transformations. Users can define custom constitutive models for alloys, and built-in Johnson-Cook or user-subroutines facilitate dynamic material response. The software also allows for precise energy deposition through Gaussian or custom beam profiles and generates complex geometries for surface texturing. The workflow includes pre-processing, simulation, and post-processing, with benefits such as predictive accuracy, resource efficiency, and versatility. Pegane-Vingadas et al. [66] used ABAQUS model to analyse the stress field developed during laser surface texturing.

ABAQUS is also used in aerospace, automotive, and biomedical sectors, ensuring precision, quality, and performance in laser-processed components. Overall, ABAQUS is an indispensable virtual platform for advancing laser texturing and processing, merging multiphysics rigor with user flexibility to drive innovation in metal alloy fabrication.

Copyright © by DILAPRO All Rights Reserved | D2.3 - Manual guide for methodologies for physically simulating AM process

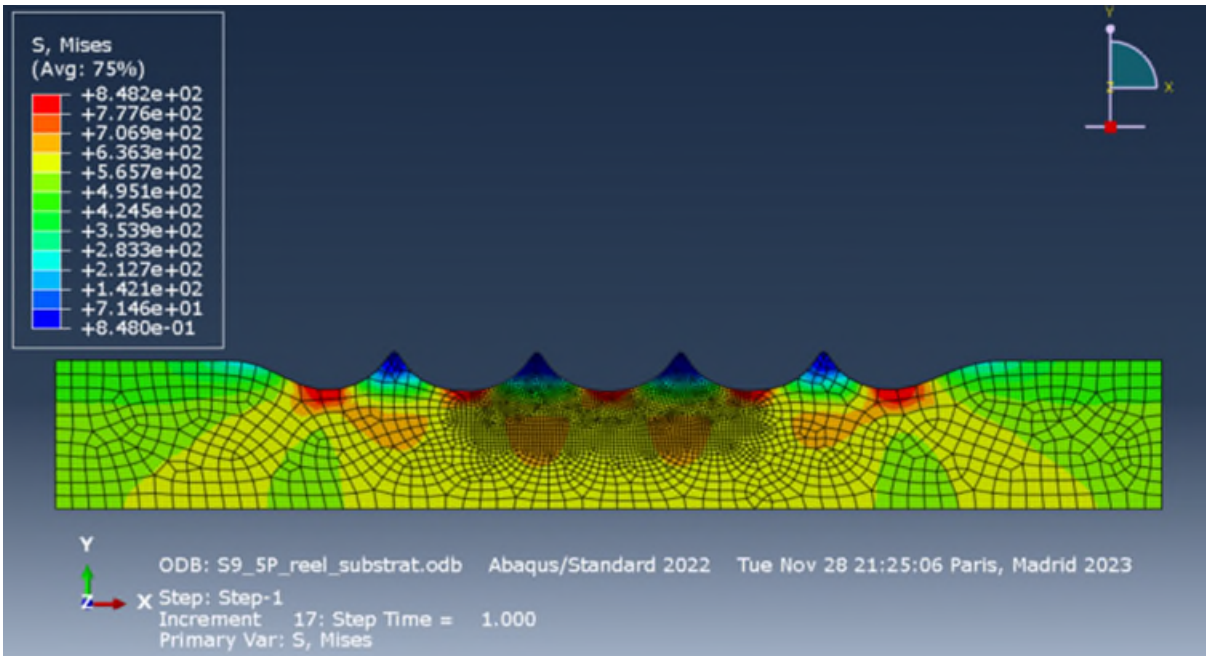


Figure 17. ABAQUS model of the stress field of laser-textured surface. [66]

4.2.4 SolidWorks

SOLIDWORKS 3D CAD software is a widely used tool for designing and preparing metal components for laser-based manufacturing processes, including laser surface texturing (LST) and additive manufacturing. It integrates parametric modeling, simulation, and manufacturing workflows to optimize surface functionalization, thermal/mechanical performance, and production efficiency for metals like steel, aluminum, and advanced alloys. SOLIDWORKS offers capabilities such as surface pattern creation, hardware integration, and etch/cut workflows. Users can design micro-textures directly on 3D models using sketches, surfaces, and sheet metal tools. Additionally, the software facilitates hardware integration through native PEM fastener libraries and Toolbox, which allow clinching hardware to be inserted with ease. Laser systems are guided by etch/cut workflows to engrave surface textures or identifiers without slicing through materials. Mesquita-Guimarães et al. have proposed SOLIDWORKS to predict the maximum temperature and heat flux within the channels fabricated using laser texturing process. Figure 18 shows the numerical results of the ideal laser geometry for alumina, Cr2AlC MAX phase, and 316 L stainless steel [34].

SOLIDWORKS has applications in metal processing, such as heat transfer enhancement, adhesive optimization, and additive manufacturing. Recent enhancements (SOLIDWORKS 2025) improve real-time collaboration and streamline assembly workflows. Future developments will further bridge CAD with laser texturing automation, particularly for renewable energy and aerospace alloys.

Copyright © by DILAPRO All Rights Reserved | D2.3 - Manual guide for methodologies for physically simulating AM process

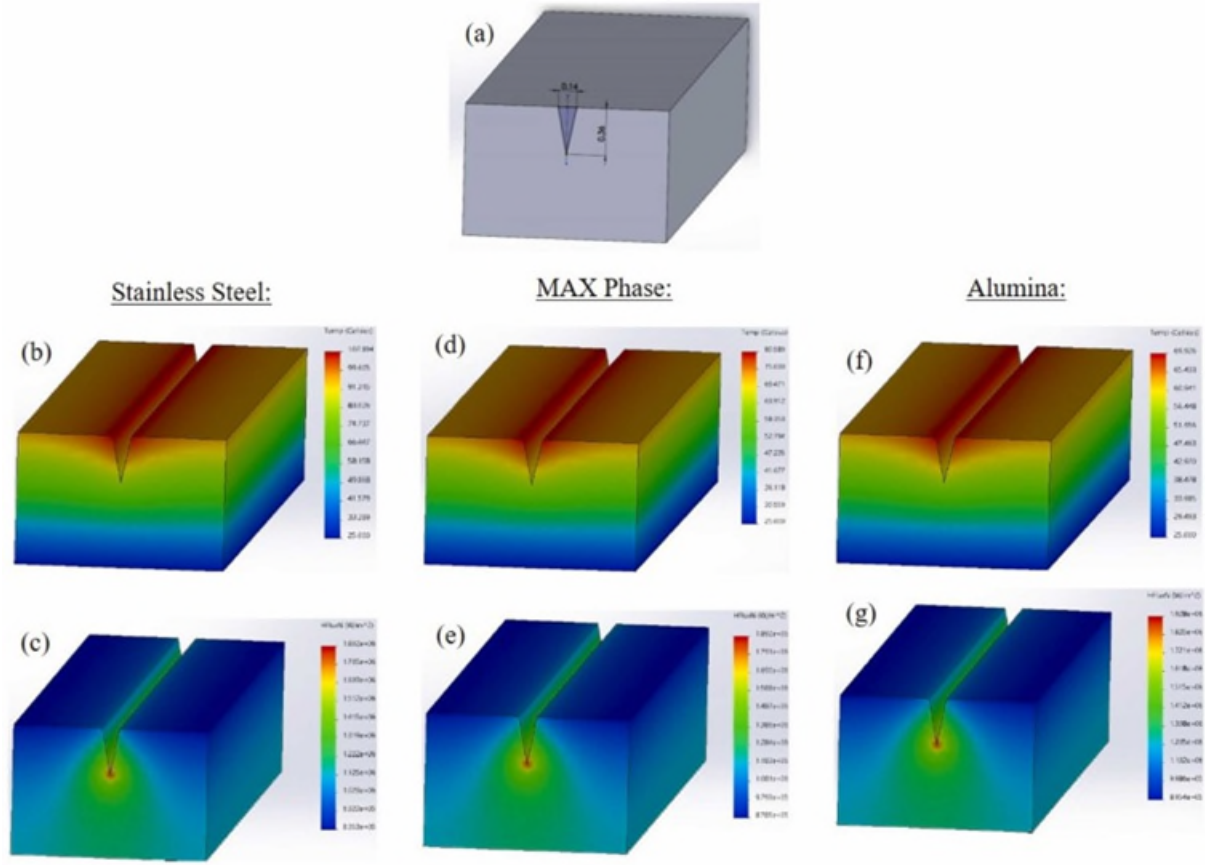


Figure 18. Simulation results of the optimized V-shape channel geometry textured with laser at air: (a) channel geometry dimensions; (b) 316 L SS maximum temperature and (c) heat flux gradient; (d) Cr2AlC maximum temperature and (e) heat flux gradient; (f) alumina maximum temperature; (g) heat flux gradient. [34]

4.2.5 OpenFOAM

OpenFOAM is an open-source computational fluid dynamics (CFD) toolbox that lets you run very accurate simulations of laser-based metal processing techniques like laser texturing, welding, additive manufacturing (L-PBF, LMD), and drilling. It uses customizable solvers to model complicated multiphysics events like how lasers interact with materials, how melt pools move, how phases change, and how defects form. The core simulation mechanisms include laser ray tracing, which discretizes laser beams into individual 'rays' that interact with the substrate. This energy deposition is computed volumetrically, accounting for multiple reflections to model keyhole formation and vaporization. Multiphase modelling is used to track gas-metal interfaces during melting/solidification, with solvers like interFoam or icoReacting Multiphase InterFoam handling immiscible fluid interactions.

OpenFOAM software also includes models for phase change and heat transfer. The enthalpy-porosity technique models melting and solidification by treating mushy areas as porous media.

Copyright © by DILAPRO All Rights Reserved | D2.3 - Manual guide for methodologies for physically simulating AM process

The software includes specific workflow models for specific activities such as laser texturing, laser welding, additive manufacturing, powder bed modelling, melt pool defect prediction, and multi-material capabilities. Aminnia et al. [67] have used OpenFOAM platform to determine the melt-pool behaviour during laser processing of stainless-steel powders. Figure 8 shows the melt pool behaviour of the experimental and simulation of process using OpenFOAM software [67]. In conclusion, OpenFOAM provides a robust, extensible framework for simulating laser-metal interactions across texturing and processing applications. Future developments aim to incorporate explicit vaporization models and machine learning for real-time parameter optimization.



(a) Experimental case at t = 10 s (b) Simulation case at t = 10 s

Figure 19. Floating packed subjected to a warm in owing water. (a) experimental result (b) simulation result. [67]

Thomae et al. [68] have used OpenFOAM to perform FEM analysis of the laser ablation process on aluminium (Al) and austenitic stainless steel (AISI 304). In this study, the craters formed on aluminium (Al) and AISI 304 stainless steel are presented in Figures 9(a) and 9(b) [68]. Experimental data are indicated by the blue and red lines. The crater profile for AISI 304 exhibits a near-rectangular shape with steep sidewalls, reflecting that the spallation mechanism removes only a minimal amount of material. The simulation results agree closely with the experimental measurements, particularly in reproducing the smooth topography. However, the simulated crater profile displays a shorter plateau region and assumes a more parabolic form, resulting in an overestimation of the minimum ablation depth. With increasing laser fluence, both experimental and simulation data reveal a transition toward a more parabolic crater morphology; the simulation accurately predicts the surface topography of the smooth sample under these conditions. Compared to the untreated surface, SEM micrographs indicate a slight increase in surface roughness. For aluminium, experimental observations show that its surface roughness exceeds that of AISI 304 in both experiment and simulation. The model tends to overpredict roughness, generating spike-like features approximately 70 nm in height and 400 nm in width. As fluence continues to rise, the crater profile on aluminium likewise becomes more parabolic mirroring the behaviour of AISI 304 until the threshold for maximum single-pulse ablation efficiency is reached.

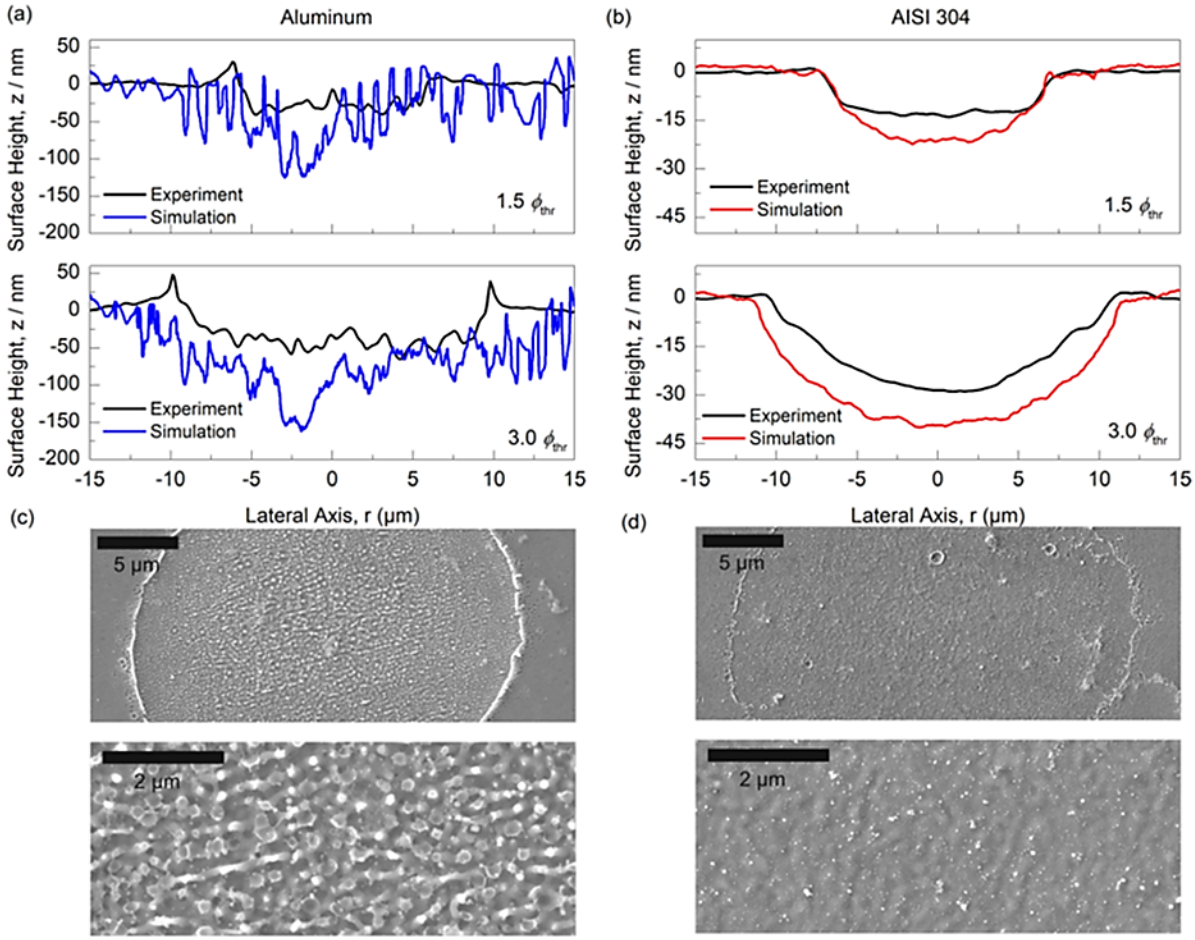


Figure 20. Panels (a) and (b) show crater cross-sections with the experimental profiles (black lines) and simulation predictions (coloured lines) at 1.5- and 3.0-times threshold fluence. Panels (c) and (d) provide SEM images at two magnifications for 3 × threshold fluence, illustrating the real surface morphology. [68].

4.2.6 Zemax

Zemax is a top-tier optical design software that aids in simulating and optimizing laser systems that are used to texture and process metals and metal alloys. It lets engineers model how beams spread out, how strong they are, and how they affect heat for precise surface changes. Zemax designs laser delivery optics to change the shape of beam profiles and guess the size of the focal spot, the depth of field and the energy distribution on the substrate. It also predicts thermal effects caused by lasers through integration with thermal and structural solvers. The software makes it easier to design DOE (Diffractive Optical Elements) for complex beam shaping. This helps to make custom phase masks that create microstructures to improve adhesion, reduce friction,

Copyright © by DILAPRO All Rights Reserved | D2.3 - Manual guide for methodologies for physically simulating AM process

or make surfaces that repel water. Zemax's workflow seamlessly integrates multiple work packages such as virtual prototyping, process validation, and multi-physics coupling. By optimizing beam control, software achieves micron level precision in texture geometry. Its predictive capabilities offer significant advantages across R&D sectors, enhancing process reliability and enabling novel surface functionalities in aerospace, automotive and medical applications. Figure 21 presents the simulation results reported by Nan et al. [69]. They employed Zemax simulation software to investigate the design complexities of a small rectangular laser source incorporating a Powell prism and cylindrical lenses. The discussion encompasses the Zemax simulation outcomes as well as analyses of laser-spot imaging, intensity distribution, and the design of various illustrative examples.

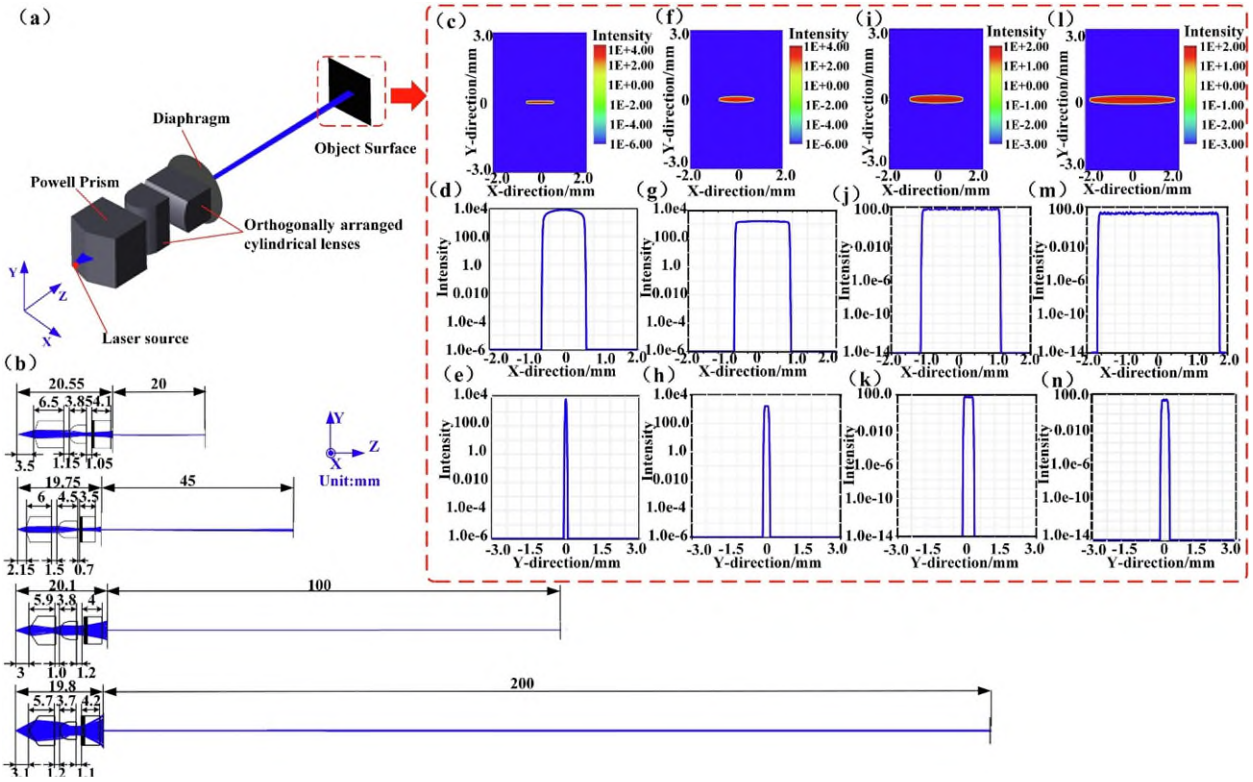


Figure 21. Small size rectangular laser source design based on combination of Powell prism and cylindrical lenses and the ZEMAX simulation results of different working references:(a) 3D structure and simulation models construction in ZEMAX ; (b) Details of the position and lens parameters in our optical simulation model; (c)-(e) showed the simulation results, the laser spot imaging on X-Y imaging plane, and the intensity distribution in X-direction was a wide flat topped Gaussian waveform, while the intensity distribution in Y-direction was a narrow flat topped Gaussian waveform; Similarly, (f)-(h), (i)-(k) and (l)-(n) were the laser imaging and intensity distribution of designed Examples. [69]

Copyright © by DILAPRO All Rights Reserved | D2.3 - Manual guide for methodologies for physically simulating AM process

4.2.7 MATLAB

MATLAB is a computational platform that enables the modelling, control, monitoring, and analysis of laser texturing and processing for metals and alloys. It integrates complex physical models, hardware interfacing, and data analytics into a cohesive workflow. Core functionalities include:

- Thermodynamic analysis using the Partial Differential Equation (PDE) Toolbox.
- Process optimization via the Optimization Toolbox and surrogate modelling.
- Beam path planning for precise laser trajectories.

Real-time control and hardware integration are provided by the Instrument Control Toolbox, which interfaces with laser systems, galvanometer scanners, motion stages, pyrometers, and CCD cameras. Closed-loop control algorithms dynamically adjust laser power and scan speed based on real-time sensor feedback. Data acquisition and post-processing encompassing surface metrology, microstructure characterization, and process validation further enhance quality assurance and deepen process understanding. This integrated platform significantly improves the development and implementation of innovative laser-based manufacturing methods for metallic components, effectively bridging the gap between theoretical models and practical systems.

In summary, MATLAB offers an efficient computational environment for modelling, controlling, monitoring, and analysing laser texturing and processing of metals and alloys by unifying advanced physical models, hardware interfacing, and data analytics into a single, extensible workflow.

4.3 Machine Learning based modelling

Machine Learning (ML) describe a broad range of Artificial Intelligence (AI) algorithms which improve their performance as predicative or generative models by learning from data. These algorithms do not require the rules and relationships governing the data to be explicitly programmed, rather forming the model directly from the data. Compared to physical simulations, ML models remove the need for careful understanding, programming, and tweaking of physical phenomenon. This may be particularly attractive for laser-material interaction processes like laser texturing, where the complex interactions and behaviour may prove challenging to theoretically model. In a manufacturing context, such as those being considered in the DILAPRO project, such empirical approaches are strongly appealing. However, to develop reliable and accurate models, ML algorithms require large training datasets and significant computation.

Supervised learning is the most commonly used ML approach for manufacturing techniques like laser texturing. In supervised learning, the algorithm is trained to predict an output from

corresponding input data. Typically, a model is "trained" to fit a set of training data, and then tested against a set of unseen validation data. The output the model is trained to predict may be class-based, such as pass/fail prediction, or regression-based, such as predicting a numerical characteristic.

In the context of laser texturing, supervised learning can be employed to map process parameters, such as laser power, pulse duration, scan speed, and repetition rate, to resulting surface characteristics like roughness, feature dimensions, or functional properties. By learning these complex input-output relationships from experimental datasets, supervised models can then model the predication of these surface parameters. Furthermore, these models may identify non-obvious correlations in the data, potentially uncovering parameter combinations that lead to improved performance. The predictive models can be used for parameter selection, or if trained with process monitoring datasets, may provide predictive quality control. These capabilities make supervised learning a powerful tool for advancing laser surface processing as an industrial technique.

4.4 Supervised and Unsupervised Learning

Machine learning techniques are broadly categorized into supervised and unsupervised learning. Supervised techniques use labelled data - where each sample or instance has a corresponding output value. These outputs could categorical labels or a numerical parameter, and these algorithms are trained to predict the output from the input data. Typical supervised algorithms include Random Forest, Logistic Regression, and Support Vector Machine [70]. Unsupervised techniques operate on unlabelled data - and uncover structure or patterns within the dataset. These techniques are useful for reducing the dimensionality of datasets, clustering of data, and anomaly detection. Typical unsupervised algorithms include k-means cluster, Principal Component Analysis (PCA), and hierarchical clustering [70].

Supervised learning is attractive for laser surface texturing, where the predication of labelled defects or final part characteristics like surface roughness from the processing parameters or in-situ monitoring data can allow modelling of the process, aid parameter selection, and provide predictive quality control. However, some application of unsupervised learning techniques to laser processing and surface textures have been reported. Mahdieh *et al.* report on the use for PCA and the clustering algorithm Density-Based Spatial Clustering of Applications with Noise (DBSCAN) to group datapoints from laser ablation monitoring data, to help distinguish good and bad ablation [71]. Mei *et al.* report on the use of unsupervised learning for automated detection of defects in textured surfaces [72]. The authors used an unsupervised Multiscale Convolutional Denoising Auto-Encoder (MSCDAE) with a Gaussian pyramid structure to analyse textures using

Copyright © by DILAPRO All Rights Reserved

image data, without manually classifying them as defective or non-defective. For repetitious textures, the algorithm could identify anomalies in the patterns of the image and thus identify defects (illustrated in Figure 22).

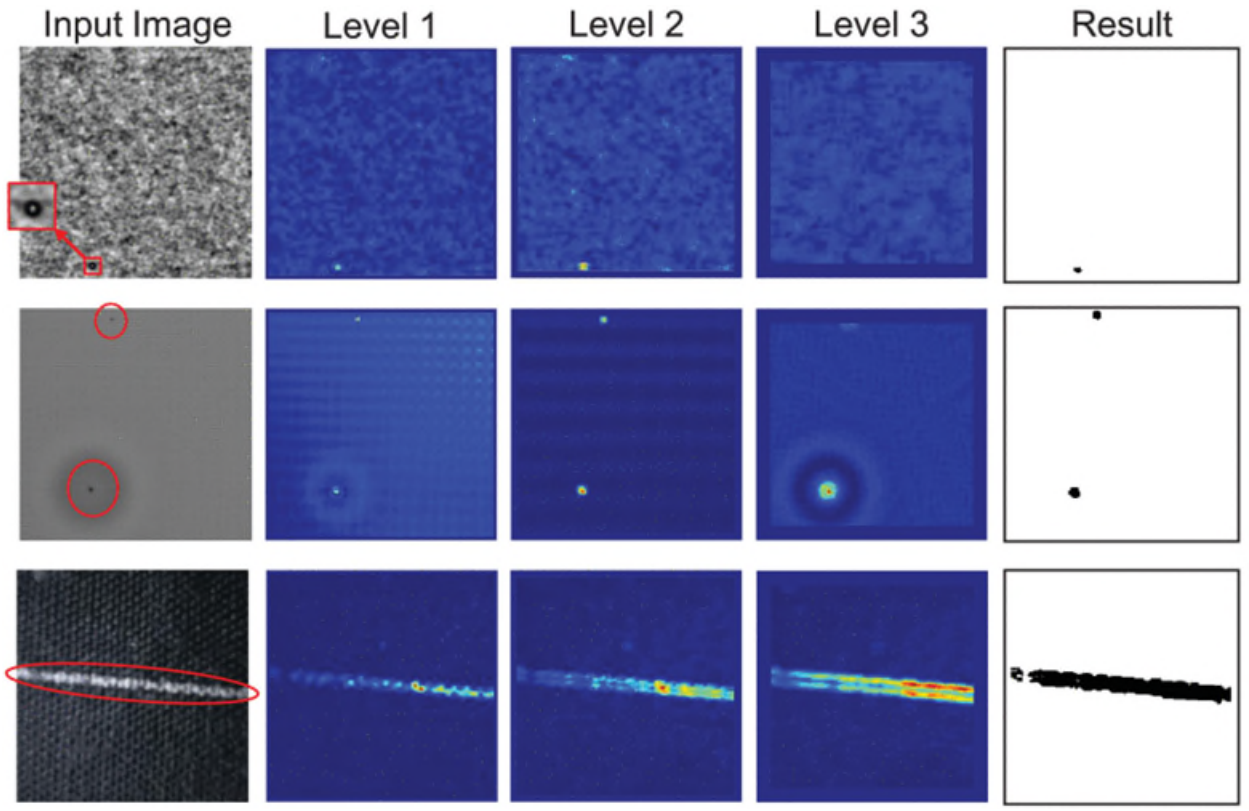


Figure 22. Detection of localised defects in surface texture using unsupervised learning algorithm (Reproduced from [72]).

Supervised learning is more suited to modelling the laser surface texturing process. As discussed, supervised algorithms can be divided in those which are classification based and those which are regression based. They can also be divided into white-box, such as Decision Trees or Linear Regression, which are interpretable, meaning their internal workings, logic, and decision-making processes are transparent and can be understood, and black-box, like deep neural networks or ensemble methods, which may achieve higher predictive performance but lack transparency and interpretability. However, despite the clear categories, there is also a spectrum of interpretability with some white-box algorithms being more interpretable than others, and some algorithms, such as Random Forest, occasionally being labelled as “grey-box” algorithms. Interpretable algorithms are more attractive for the DILAPRO project and softwares than black boxes, as they will give greater insight into the process and the relationship between process parameters and quality factors, which may be useful in developing process control.

Copyright © by DILAPRO All Rights Reserved

4.4.1 Supervised Regression-based Algorithms

Supervised regression-based machine learning algorithms are attractive for modelling of processes like laser texturing, due to their ability to be trained to predict final properties from process data without the programming of a theoretical model of the physical process. This class of algorithm is being used in the development of the DILAPRO software. Training an algorithm using the process parameters and monitoring data as inputs, and the various quality factors that are of interest for different LST applications as outputs, creates an empirical model which can predict the final part properties before, and as, a texture is produced. This enables intelligent parameter selection - choosing the parameters that predict the best quality surface - and in-process predicative quality control - predicting the quality factors from the monitoring data to ensure that the processing is delivering the desired results. In this sub-section, ML modelling approaches are reviewed.

Bañon *et al.* illustrate the usefulness of machine learning, by comparing the use of an ML approach to a conventional statistical approach [73]. Response Surface Modelling (RSM) was used to conventionally analyse the roughness and wettability of surfaces textured using a Rofin Easymark F20 Ytterbium laser, and compared to ML modelling using an Artificial Neural Network (ANN). The RSM approach used a second order polynomial model with good accuracy, but was out-performed by the ANN which predicted all four roughness parameters (*Ra*, *Rt*, *Rz*, and *Rv*) with accuracies of 81 - 98% for unseen validation data. The ANN can predict all four parameters from one model (while the RSM can only predict one output parameter from a single model). A comparison of the accuracy for the two methods is shown in Figure 23. This illustrates the ability of machine learning approaches to improve predictive accuracy.

Copyright © by DILAPRO All Rights Reserved

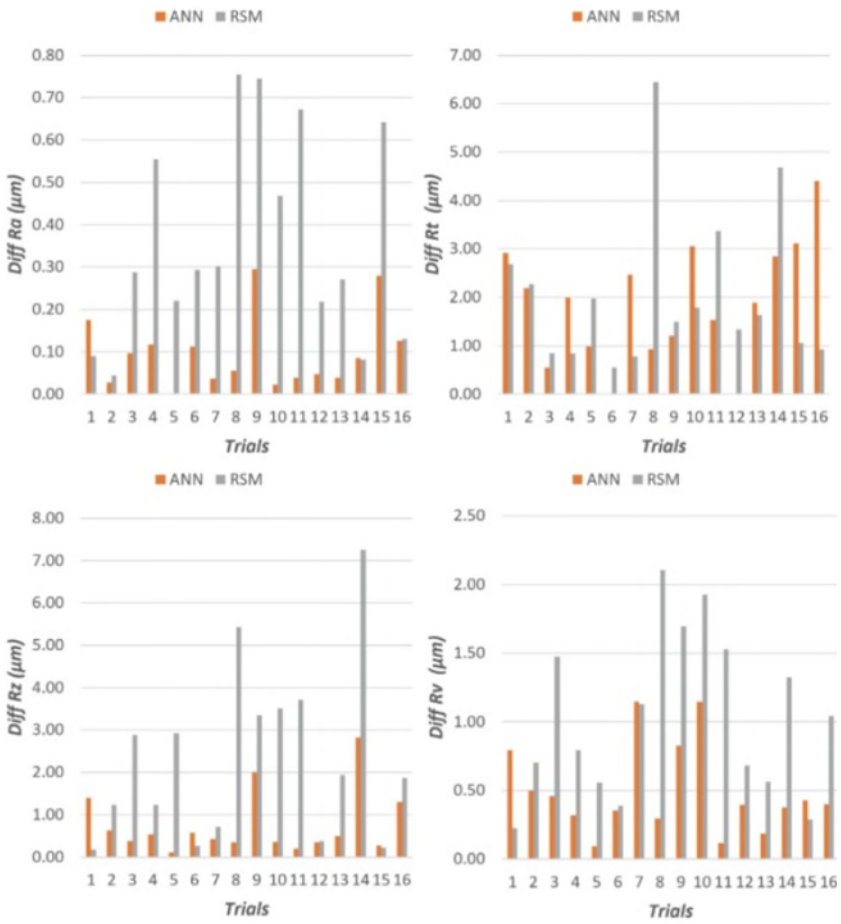


Figure 23. Differences in absolute values between the results obtained by the predictive response surface models (grey) and neural networks (orange) with respect to the variables: a) Ra; b) Rt; c) Rz; d) Rv (Reproduced from [73]).

Steege *et al.* also applied ML to prediction of the surface roughness, in this case the Sa, in laser texturing [74]. The authors applied Random Forest and ANN achieving similar R^2 values of ~0.79 for 316L and ~0.91 for Stavax. While ANNs are considered black-box algorithms, Random Forest offers some interpretability. The most important feature for prediction in both materials was the accumulated fluence during texturing, followed by the pulse energy and power for 316L, and the pulse energy and scanning speed for Stavax. This illustrates how explainable AI can be used in modelling of processes to gain insight into the relationship of the inputs and outputs, which is highly attractive for the DILAFACT and DILACERT softwares.

Moles *et al.* explored the effectiveness of multiple different ML regression algorithms, including ANN, for predictive modelling of the depth of the channel in femtosecond laser texturing [75]. The models they applied were a Decision Trees (DT), Random Forest (RF), Gaussian Process (GP), Support Vector Machines (SVM), K-nearest Neighbours (KNN), and Artificial Neural Network

Copyright © by DILAPRO All Rights Reserved | D2.3 - Manual guide for methodologies for physically simulating AM process

(ANN) algorithm. The ANN performed the best in accuracy (R^2 of 0.79-0.99) for predicting the depth of lines and dimples across the three selected materials (Steel, TiN, and TiCN), with SVM and GP performing with matching accuracy to ANN in some cases and just slightly lower in others.

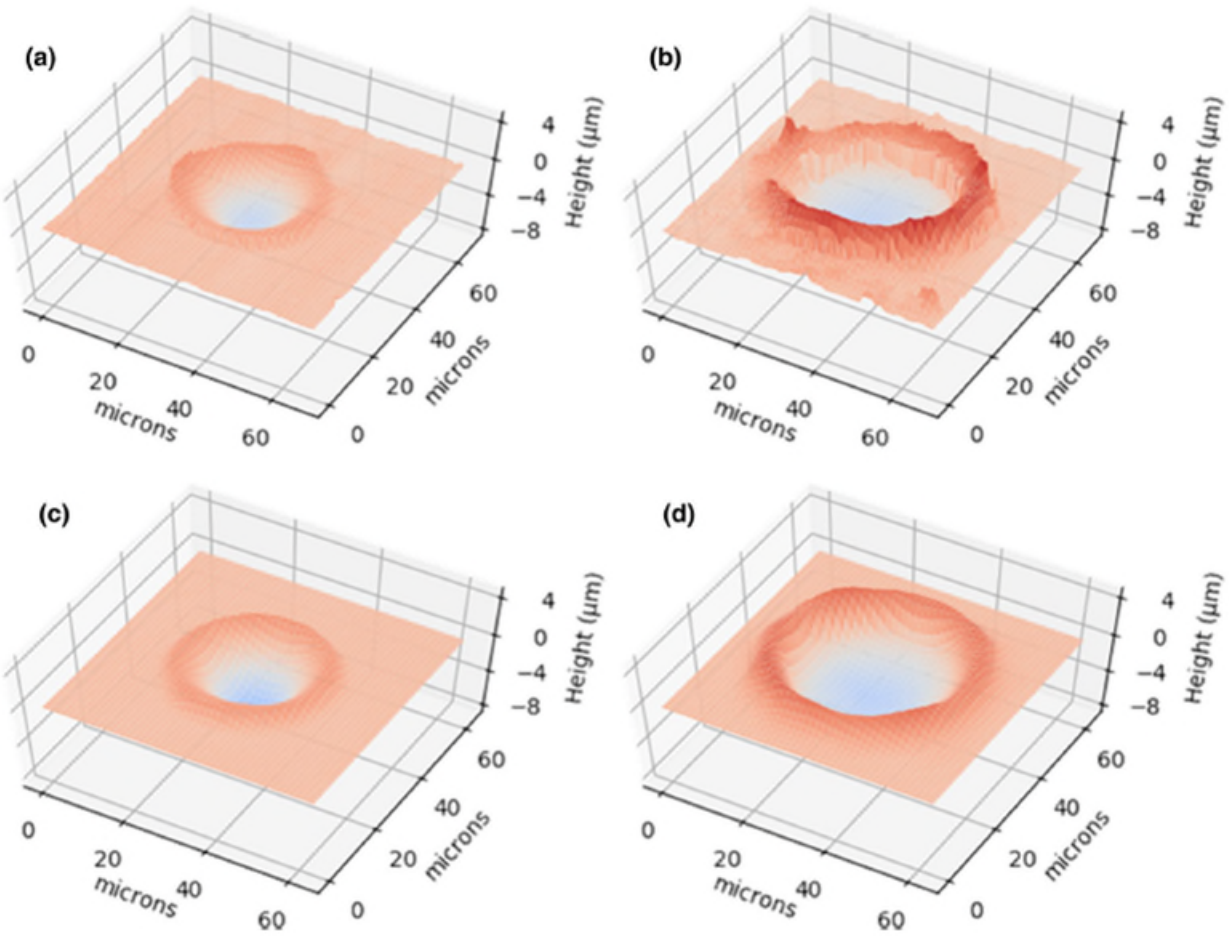


Figure 24. Visualisation of real and predicted laser ablated surface. (a) and (b) are the measured surface laser machined with repetition rate of 10 kHz & pulse energy 47.17 uJ for 200 pulses, and 1200 kHz & 12.41 uJ for 100 pulses, respectively. (c) is the Generative Adversial Network (GAN) prediction for the parameters of (a), and (d) is the GAN prediction for the parameters of (b) (Reproduced from [76]).

Machine learning has also been applied for predictive modelling visualisation of laser processed surface topography. McDonnell *et al.* used a Generative Adversarial Network (GAN) to generated predicted 3D surface profiles for laser ablated surfaces from the process parameters [76]. The GAN process uses two competing networks, a generator and a discriminator, to generate images and compare to real data, to improve the performance of both over time. The GAN was trained on experimental data and was able to produce approximations of the real resultant craters (see

Copyright © by DILAPRO All Rights Reserved | D2.3 - Manual guide for methodologies for physically simulating AM process

Figure 24). The generated craters are lacking in the detail and stochasticity of the spikier real craters, but serve to give an accurate “averaged” crater with accurate height and width. Visual simulation of final part properties may be more "user-friendly" and quickly interpretable than purely numerical predictions, and thus a similar approach for texture patches could be a consideration for later addition to the DILAFACT software.

While exploration of laser texturing modelling with machine learning has been limited to date, these reports indicate the strong performance of these algorithms in predictive modelling, with strong potential for use in defect detection and process control. The benefits highlighted above are why explainable regression-based supervised learning algorithms have been identified as a key modelling approach for the DILACERT software.

4.5 Conclusion to Part 2

Laser Surface Texturing (LST) is a powerful and versatile technology for precisely engineering material surfaces to achieve tailored functional properties across diverse engineering sectors. The advent of ultrafast lasers, particularly femtosecond lasers, has revolutionized this field by enabling unprecedented precision and minimal thermal impact. This capability allows for the direct fabrication of intricate micro- and nanostructures such as spikes, laser-induced periodic surface structures (LIPSS), and nanopillars without significant heat-affected zones, melting, or recast layers, thereby overcoming limitations inherent in traditional thermal-ablation methods. The physical complexity of the LST process makes simulation and modeling difficult, but essential. In this Deliverable, we have reviewed physical simulation and machine learning modeling for LST. Understanding of these is key for implementation in the DILAFACT and DILACERT softwares, where modeling will be used to allow users to make intelligent choices in selecting their parameters based on their application and desired surface, and also enable predictive quality control.

The following key insights emerge from this study:

- **Versatility of LST**: LST provides a flexible means of engineering material surfaces to exhibit specific functional properties.
- **Precision with ultrafast lasers**: The use of femtosecond lasers affords high spatial resolution and minimal thermal damage, enabling the creation of complex micro- and nanostructures.
- **Enhanced tribological performance**: Controlled surface features produced by LST reduce friction and improve wear resistance.

- **Wettability control**: LST permits precise manipulation of surface wettability, yielding functional coatings suited to marine, automotive, and biomedical applications.
- **Thermal-property optimization**: Surface texturing enhances heat-flux management, condensation heat transfer, and spectral emissivity for high-temperature environments.
- **Reliance on computational modelling**: Process development leverages advanced simulation tools such as COMSOL Multiphysics, ANSYS, and custom MATLAB or Python models to predict outcomes and optimize parameters.
- **Cost and time reduction**: Simulation frameworks decrease experimental effort and accelerate the identification of optimal processing conditions.
- **Opportunity of ML:** Machine learning's ability to produce empirical models without complex theoretical understanding of dynamic physical processes can achieve impressive results in predicting texture properties.
- **Cross-sector significance**: LST's ability to tailor surface characteristics is increasingly valuable in manufacturing, aerospace, defense, and healthcare.
- **Outlook**: Ongoing advancements in laser technology and simulation methodologies are expected to further improve precision and efficiency, and to expand the range of applications for surface-engineered materials.

Bibliography

1. H. Ferguson. The Physical Simulation of Continuous Steel Processes. *JOM.* 40 (1988) 14–16. DOI: 10.1007/BF03257975
2. F. Siciliano, B.J. Allen, S.F. Rodrigues, J.J. Jonas. *Mater Sci Forum*. 941 (2018) 438-442.
3. L. Poloczek, L. Rauch, M. Wilkus, D. Bachniak, W. Zalecki, V. Pidvysotsk'yy, R. Kuziak, M. Pietrzyk. Physical and Numerical Simulations of Closed Die Hot Forging and Heat Treatment of Forged Parts. *Materials.* 14 (2021) 15. DOI: 10.3390/ma14010015.
4. F. Kellogg, E. Vasilev, A. Kudzal, J. Taggart-Scarff, J. Marsico, M. Knezevic, B. McWilliams. Physical simulations of heat-affected zone microstructures to compare weldability characteristics of additively manufactured and wrought 17-4 stainless steel. *Mater Charact*. 185 (2022) 111714. DOI: 10.1016/j.matchar.2021.111714.

Copyright © by DILAPRO All Rights Reserved

5. A.R. Eivani, J. Zhou. Application of physical and numerical simulations for interpretation of peripheral coarse grain structure during hot extrusion of AA7020 aluminum alloy. *J Alloys Compd*. 725 (2017) 41-53. DOI: 10.1016/j.jallcom.2017.06.297.

6. M. Rahimian, S. Milenkovic, L. Maestro, A.E.R. de Azua, I. Sabirov. Physical Simulation of Investment Casting of Complex Shape Parts. *Metall Mater Trans A*. 46 (2015) 2227-2237. DOI: 10.1007/s11661-015-2815-6.

7. l. Büßenschütt, P. Köhnen, F. Kies, S. Koß, J.H. Schleifenbaum, C. Haase. High-speed direct energy deposition as a high-throughput design tool for laser-based additive manufacturing. *Add Manuf Lett*. 8 (2024) 100188. DOI: 10.1016/j.addlet.2023.100188.

8. J. Jeong, S. Webster, S. Liao, J.E. Mogonye, K. Ehmann, J. Cao. Cooling rate measurement in directed energy deposition using PDPT. *Add Manuf Lett*. 3 (2022) 100101. DOI: 10.1016/j.addlet.2022.100101.

9. K. Kosiba, T. Gustmann, J.T. Kim, J. Seok, J. Jung, L. Beyer, S. Scudino, L. Giebeler, J. Han, K.J. Hufenbach. Experimental cooling rates during high-power LPBF at varying processing conditions. *J Alloys Compd.* 967 (2023) 171773. DOI: 10.1016/j.jallcom.2023.171773.

10. M.P.P. Sotiriou, J.S.S. Aristeidakis, M.I.T.T. Tzini, I. Papadioti, G.N. Haidemenopoulos, N. Aravas. Microstructural and Thermomechanical Simulation of the Additive Manufacturing Process in 316L Austenitic Stainless Steel. *Mater Proc.* 3 (2021) 20. DOI: 10.3390/IEC2M-09237.

11. E.A. Lass, M.R. Stoudt, M.E. Williams. Formation of the Ni3Nb δ-Phase in Stress-Relieved Inconel 625 Produced via Laser Powder-Bed Fusion Additive Manufacturing. *Metall Mater Trans A*. 48 (2017) 5547–5558. DOI: 10.1007/s11661-017-4304-6.

12. Y. M. Wang *et al.*, Additively manufactured hierarchical stainless steels with high strength and ductility, *Nat Mater*. 17 (2018) 63–70. DOI: 10.1038/NMAT5021.

13. A. Cholkar, R. McCann, G. Perumal, S. Chatterjee, M. Swayne, D. Kinahan, D. Brabazon, Advances in laser-based surface texturing for developing antifouling surfaces: A comprehensive review, *Appl Surf Sci Adv*. 18 (2023) 100513. https://doi.org/10.1016/j.apsadv.2023.100513.

14. A. Ancona, C. Gaudiuso, A. Volpe, F.P. Mezzapesa, C. Putignano, G. Carbone, Laser surface texturing for superhydrophobic, icephobic and friction reduction functionalization, *IOP Conf Ser Mater Sci Eng*. 1296 (2023) 012042. https://doi.org/10.1088/1757-899X/1296/1/012042.

15. A.A. Khalil, X. Sedao, S. Papa, P. Claudel, A. Klos, T. Itina, N. Attik, A. Guignandon, V. Dumas, Ultrafast laser processing of nanostructured patterns for the control of cell adhesion and migration on titanium alloy, in: 2021 Conference on Lasers and Electro-

Copyright © by DILAPRO All Rights Reserved | D2.3 - Manual guide for methodologies for physically simulating AM process

Optics Europe & European Quantum Electronics Conference (CLEO/Europe-EQEC), *IEEE*, 2021: pp. 1–1. https://doi.org/10.1109/CLEO/Europe-EQEC52157.2021.9541931.

16. A. Bharatish, S. Soundarapandian, Influence of Femtosecond Laser Parameters and Environment on Surface Texture Characteristics of Metals and Non-Metals – State of the Art, *Lasers Manuf Mater Proc*. 5 (2018) 143–167. https://doi.org/10.1007/s40516-018-0059-1.
17. G. Chen, J. Qiao, Femtosecond-laser-enabled simultaneous figuring and finishing of glass with a subnanometer optical surface, *Opt Lett*. 47 (2022) 3860. https://doi.org/10.1364/OL.467413.
18. A. Čermák, K. Simonović, A. Bondarev, P. Kožmín, Š. Syrovátka, T. Polcar, J. Syrovátka, Femtosecond laser texturing of DLC-based coatings by DLW method with sub-micrometer precision, *Int J Adv Manuf Tech*. 121 (2022) 8479–8494. https://doi.org/10.1007/s00170-022-09855-0.
19. I. Shivakoti, G. Kibria, R. Cep, B.B. Pradhan, A. Sharma, Laser Surface Texturing for Biomedical Applications: A Review, *Coatings*. 11 (2021) 124. https://doi.org/10.3390/coatings11020124.
20. G. Padmanabham, R. Bathe, Laser Materials Processing for Industrial Applications, *Proceedings of the National Academy of Sciences, India Section A: Physical Sciences*. 88 (2018) 359–374. https://doi.org/10.1007/s40010-018-0523-5.
21. S. Nikumb, R. Bathe, G.K. Knopf, Laser microprocessing technologies for automotive, flexible electronics, and solar energy sectors, in: E.W. Reutzel (Ed.), 2014: p. 918005. https://doi.org/10.1117/12.2064279.
22. S.P. Murzin, C. Stiglbrunner, Fabrication of Smart Materials Using Laser Processing: Analysis and Prospects, *Appl Sci*. 14 (2023) 85. https://doi.org/10.3390/app14010085.
23. E. Khalkhal, M. Rezaei-Tavirani, M.R. Zali, Z. Akbari, The Evaluation of Laser Application in Surgery: A Review Article., *J Lasers Med Sci*. 10 (2019) S104–S111. https://doi.org/10.15171/jlms.2019.S18.
24. V. Narayanan, R. Singh, D. Marla, A 3D Computational Model of Nanosecond Pulsed Laser Texturing of Metals for Designing Engineered Surfaces, *J Manuf Sci Eng*. 146 (2024) 051006. https://doi.org/10.1115/1.4064833.
25. H.X. Liu, Y.X. Chen, X. Wang, X.X. Meng, Y.H. Fu, L. Cai, Numerical Simulation of Laser Surface Micro-Texturing, *Mater Sci Forum*. 575–578 (2008) 678–683. https://doi.org/10.4028/www.scientific.net/MSF.575-578.678.

Copyright © by DILAPRO All Rights Reserved | D2.3 - Manual guide for methodologies for physically simulating AM process

26. H. Ebrahimi Orimi, S. Jagadeesh, S. Narayanswamy, Experimental investigation of texturing complex geometry using high repetition nano laser and comparison with the simulated COMSOL model, in: U. Klotzbach, K. Washio, R. Kling (Eds.), Laser-Based Micro- and Nanoprocessing XII, SPIE, 2018: p. 72. https://doi.org/10.1117/12.2298770.

27. E.R. Moldovan, C. Concheso Doria, J.L. Ocaña, L.S. Baltes, E.M. Stanciu, C. Croitoru, A. Pascu, I.C. Roata, M.H. Tierean, Wettability and Surface Roughness Analysis of Laser Surface Texturing of AISI 430 Stainless Steel, *Materials*. 15 (2022) 2955. https://doi.org/10.3390/ma15082955.

28. A.Y. Escudero-Ornelas, E. Davey, A. Valera-Medina, S. Bigot, D. Badhuri, A Study on the Surface Chemistry of Laser Textured Parts, in: Proceedings of the Cardiff University Engineering Research Conference 2023, Cardiff University Press, 2024: pp. 128–132. https://doi.org/10.18573/conf1.ad.

29. M. Isa Rahim, S.N. Aqida, M.S. Salwani, S. Ahmad Syarizan, Enhancing Surface Hydrophobicity of AISI 304 Stainless Steel via Laser Texturing, *J Phys Conf Ser*. 2933 (2025) 012006. https://doi.org/10.1088/1742-6596/2933/1/012006.

30. R. Fürbacher, G. Grünsteidl, A. Otto, G. Liedl, Chemical and UV Durability of Hydrophobic and Icephobic Surface Layers on Femtosecond Laser Structured Stainless Steel, *Coatings.* 14 (2024) 924. https://doi.org/10.3390/coatings14080924.

31. P. Lorenz, J. Zajadacz, L. Streisel, M. Ehrhardt, R. Morgenstern, T. Lampke, G. Hommes, S. Peter, K. Zimmer, Mechanical Abrasion of Laser-Machined Highly Hydrophobic Stainless Steel Surface Depending on Surface Topography, *Phys Stat Solid (a).* 221 (2024) 2300482. https://doi.org/10.1002/pssa.202300482.

32. J. Zhang, D. Yang, A. Rosenkranz, J. Zhang, L. Zhao, C. Song, Y. Yan, T. Sun, Laser Surface Texturing of Stainless Steel – Effect of Pulse Duration on Texture's Morphology and Frictional Response, *Adv Eng Mater*. 21 (2019) 1801016. https://doi.org/10.1002/adem.201801016.

33. V. Kumar, R. Verma, H.K. Bairwa, Fabrication of superhydrophobic surfaces by laser surface texturing and autoxidation, *J Electrochem Sci Eng*. 12 (2022) 639-649. https://doi.org/10.5599/jese.1260.

34. J. Mesquita-Guimarães, N.M. Ferreira, R.M.S. Reis, J. Gonzalez-Julian, J. Pinho-da-Cruz, Laser surface texturing and numerical simulation of heat flux on Cr2AlC MAX phase heat exchangers, *J Eur Ceram Soc*. 43 (2023) 5894–5903. https://doi.org/10.1016/j.jeurceramsoc.2023.06.031.

35. Y. Seid Ahmed, J. M. DePaiva, F. L. Amorim, R. D. Torres, W. de Rossi, S. C. Veldhuis, Laser surface texturing and characterization of austenitic stainless steel for the improvement

of its surface properties, *Int J Adv Manuf Tech.* 115 (2021) 1795–1808. https://doi.org/10.1007/s00170-021-07284-z.

36. K.Y.M. Iqbal, D.Z. Segu, H. Pyung, J.H. Kim, S.S. Kim, Surface Texturing for Low Friction Mechanical Components, *Journal of the Korean Society of Tribologists and Lubrication Engineers*. 31 (2015) 287–293. https://doi.org/10.9725/kstle.2015.31.6.287.
37. J. Zhang, D. Yang, A. Rosenkranz, J. Zhang, L. Zhao, C. Song, Y. Yan, T. Sun, Laser Surface Texturing of Stainless Steel – Effect of Pulse Duration on Texture's Morphology and Frictional Response, *Adv Eng Mater*. 21 (2019) 1801016. https://doi.org/10.1002/adem.201801016.
38. V. Mandal, V. Tiwari, M. Sarkar, S.S. Singh, J. Ramkumar, Numerical and experimental study of micro-convex dimple developed by laser additive manufacturing for surface applications, *Manufacturing Technology Today (MTT)*. 22 (2023) 45–50. https://doi.org/10.58368/MTT.22.1.2023.45-50.
39. B.S. Yilbas, H. Ali, N. Al-Aqeeli, C. Karatas, Laser treatment of Inconel 718 alloy and surface characteristics, *Opt Laser Tech*. 78 (2016) 153–158. https://doi.org/10.1016/j.optlastec.2015.11.006.
40. A. Marques, A. Cunha, S. Faria, F.S. Silva, O. Carvalho, Predictive models on the influence of laser texturing parameters on the Inconel 718 surface by using Nd: YVO4 laser, *Opt Laser Tech*. 154 (2022) 108320. https://doi.org/10.1016/j.optlastec.2022.108320.
41. S. Canacoo, E. Contreras Lopez, O. Coronel, F. Ahmed, J. Li, A. Srivastava, Ultrafast Laser Ablation of Inconel 718 for Surface Improvement, *Manuf Lett*. 33 (2022) 410–414. https://doi.org/10.1016/j.mfglet.2022.07.054.
42. V. Mandal, V. Tiwari, M. Sarkar, S.S. Singh, J. Ramkumar, Numerical and experimental study of micro-convex dimple developed by laser additive manufacturing for surface applications, *Manufacturing Technology Today (MTT)*. 22 (2023) 45–50. https://doi.org/10.58368/MTT.22.1.2023.45-50.
43. A.H.A. Lutey, L. Gemini, L. Romoli, G. Lazzini, F. Fuso, M. Faucon, R. Kling, Towards Laser-Textured Antibacterial Surfaces, *Sci Rep*. 8 (2018) 10112. https://doi.org/10.1038/s41598-018-28454-2.
44. I. Adijāns, L. Lazov, M. Ilieva, M.P. Nikolova, Investigation of the change in wettability properties and corrosion behavior of AISI 304 after laser surface texturing, *J Phys Conf Ser*. 2487 (2023) 012040. https://doi.org/10.1088/1742-6596/2487/1/012040.
45. A. Daskalova, L. Angelova, Design of Surfaces with Persistent Antimicrobial Properties on Stainless Steel Developed Using Femtosecond Laser Texturing for Application in "High Traffic" Objects, *Nanomater.* 13 (2023) 2396. https://doi.org/10.3390/nano13172396.

Copyright © by DILAPRO All Rights Reserved | D2.3 - Manual guide for methodologies for physically simulating AM process

46. V. Mandal, S. Sharma, S.S. Singh, J. Ramkumar, Laser Surface Texturing in Powder Bed Fusion: Numerical Simulation and Experimental Characterization, *Metal Mater Int.* 28 (2022) 181–196. https://doi.org/10.1007/s12540-021-01072-w.

47. D. Lou, G. Lu, T. Li, B. Wang, S. Mei, Q. Liu, J. Cheng, D. Liu, Direct laser selective texturing to improve stainless steel surface condensation heat transfer without any chemical treatment, in: Y. Sano, M. Hong, R. Xiao, J. Yao (Eds.), *Advanced Laser Processing and Manufacturing IV, SPIE*, 2020: p. 14. https://doi.org/10.1117/12.2573573.

48. J. Li, D. Xiong, H. Wu, Y. Zhang, Y. Qin, Tribological properties of laser surface texturing and molybdenizing duplex-treated stainless steel at elevated temperatures, *Surf Coat Tech*. 228 (2013) S219–S223. https://doi.org/10.1016/j.surfcoat.2012.06.002.

49. S.A. Zolotovskaya, S. Wackerow, H. Neupert, M.J. Barnes, L.V. Cid, B. Teissandier, A.T.P. Fontenla, A. Abdolvand, High-performance thermal emitters based on laser-engineered metal surfaces, *Opt Mater Express*. 10 (2020) 622. https://doi.org/10.1364/OME.381668.

50. E.D. Kozłowska, M. Szkodo, T. Muszyński, P. Adamska, The Laser Processing of the Stainless-Steel Surface Layer of a Heat Exchanger Membrane in Order to Enhance Its Heat Transfer Coefficient, *Coatings.* 15 (2025) 72. https://doi.org/10.3390/coatings15010072.

51. A. Marques, A. Cunha, S. Faria, F.S. Silva, O. Carvalho, Predictive models on the influence of laser texturing parameters on the Inconel 718 surface by using Nd: YVO4 laser, *Opt Laser Tech.* 154 (2022) 108320. https://doi.org/10.1016/j.optlastec.2022.108320.

52. A. Temmler, M. Küpper, M.A. Walochnik, A. Lanfermann, T. Schmickler, A. Bach, T. Greifenberg, O. Oreshkin, E. Willenborg, K. Wissenbach, R. Poprawe, Surface structuring by laser remelting of metals, *J Laser Appl*. 29 (2017) 012015. https://doi.org/10.2351/1.4972414.

53. D. Redka, J. Vollmann, J. Winter, M. Schmidt, J. Minár, H.P. Huber, P. Schmid, Improving FEM-based solid mechanics simulations for ultrashort pulse laser ablation by integrating an equation of state and material separation, *Int J Heat Mass Transf*. 241 (2025) 126714. https://doi.org/10.1016/j.ijheatmasstransfer.2025.126714.

54. K. Zeng, D. Pal, H.J. Gong, N. Patil, B. Stucker, Comparison of 3DSIM thermal modelling of selective laser melting using new dynamic meshing method to ANSYS, *Mat Sci Tech*. 31 (2015) 945–956. https://doi.org/10.1179/1743284714Y.0000000703.

55. S. Limrungruengrat, A. Chaikittiratana, S. Pornpeerakeat, T. Chantrasmi, Thermo-mechanical finite element simulation and validation of rubber curing process, *J Mech Sci Tech*. 36 (2022) 3039–3046. https://doi.org/10.1007/s12206-022-0534-7.

56. A. Miloshevsky, S.S. Harilal, G. Miloshevsky, A. Hassanein, Dynamics of plasma expansion and shockwave formation in femtosecond laser-ablated aluminum plumes in argon gas at

atmospheric pressures, *Phys Plasmas*. 21 (2014) 043111. https://doi.org/10.1063/1.4873701.

57. M. Naeem, T. Imran, ZEMAX Simulations and Experimental Validation of Laser Interferometers, *Photonics*. 12 (2025) 206. https://doi.org/10.3390/photonics12030206.
58. L. V. Zhigilei, B.J. Garrison, Microscopic mechanisms of laser ablation of organic solids in the thermal and stress confinement irradiation regimes, *J Appl Phys*. 88 (2000) 1281–1298. https://doi.org/10.1063/1.373816.
59. H.O. Jeschke, M.E. Garcia, K.H. Bennemann, Theory for the Ultrafast Ablation of Graphite Films, *Phys Rev Lett*. 87 (2001) 015003. https://doi.org/10.1103/PhysRevLett.87.015003.
60. L. Jiang, H.L. Tsai, Prediction of crater shape in femtosecond laser ablation of dielectrics, *J Phys D Appl Phys.* 37 (2004) 1492–1496. https://doi.org/10.1088/0022-3727/37/10/012.
61. J. Xu, D. Xue, O. Gaidai, Y. Wang, S. Xu, Molecular Dynamics Simulation of Femtosecond Laser Ablation of Cu50Zr50 Metallic Glass Based on Two-Temperature Model, *Processes*. 11 (2023) 1704. https://doi.org/10.3390/pr11061704.
62. L. Peng, M. Li, P. Wang, M. He, C. Zhou, H. Zhang, S. Chen, Numerical Simulation of Ultra-Short Pulse Laser Ablation Based on Comsol, *SSRN Electronic Journal* (2022). https://doi.org/10.2139/ssrn.4280224.
63. B. Wang, Y. Huang, J. Jiao, H. Wang, J. Wang, W. Zhang, L. Sheng, Numerical Simulation on Pulsed Laser Ablation of the Single-Crystal Superalloy Considering Material Moving Front and Effect of Comprehensive Heat Dissipation., *Micromachines.* 12 (2021) 225. https://doi.org/10.3390/mi12020225.
64. N. Deshmukh, A. Rajurkar, O. Kolekar, R. Mule, S. Chinchanikar, Thermal modeling of laser surface micro-texturing: Investigation on effects of laser parameters on dimple-texture dimensions and aspect ratio, *Mater Today Proc*. 46 (2021) 8374–8380. https://doi.org/10.1016/j.matpr.2021.03.420.
65. H.X. Liu, Y.X. Chen, X. Wang, X.X. Meng, Y.H. Fu, L. Cai, Numerical Simulation of Laser Surface Micro-Texturing, *Mater Sci Forum*. 575–578 (2008) 678–683. https://doi.org/10.4028/www.scientific.net/MSF.575-578.678.
66. E. Pegane-Vingadas, M. Chaussumier, A. Soveja, S. Costil, Effect of Laser Texturing in Thermal Spraying on the Fatigue Life of the Ti-6Al-4V Alloy, *J Thermal Spray Tech*. 34 (2025) 714–734. https://doi.org/10.1007/s11666-024-01912-2.
67. N. Aminnia, A. Estupinan Donoso, B. Peters, Developing a DEM-Coupled OpenFOAM solver for multiphysics simulation of additive manufacturing process, in: 8th European

Copyright © by DILAPRO All Rights Reserved

Congress on Computational Methods in Applied Sciences and Engineering, CIMNE, 2022. https://doi.org/10.23967/eccomas.2022.084.

68. N. Thomae, M. Stabroth, J. Vollmann, M. Döring, D. Redka, H.P. Huber, M. Schmidt, From surface roughness to crater formation in a 2D multi-scale simulation of ultrashort pulse laser ablation, *Appl Phys A*. 131 (2025) 27. https://doi.org/10.1007/s00339-024-08064-8.

69. Z. Nan, Z. Feng, Y. Wang, C. Gong, Z. Pan, W. Tao, An optimization method of rough surface adapted small rectangular LD laser source based on combination of Powell prism and cylindrical lenses, *Measurement*. 215 (2023) 112859. https://doi.org/10.1016/j.measurement.2023.112859.

70. Y. Seid Ahmed, Optimizing Femtosecond Texturing Process Parameters Through Advanced Machine Learning Models in Tribological Applications, *Lubricants*. 12 (2024) 1–24. https://doi.org/10.3390/lubricants12120454.

71. M. Samimi, H. Hosseinlaghab, É. McCarthy, P.J. McNally, Multi-Messenger Radio Frequency and Optical Diagnostics of Pulsed Laser Ablation Processes, *J Manuf Mater Proc*. 6 (2022) 106. https://doi.org/10.3390/jmmp6050106.

72. S. Mei, H. Yang, Z. Yin, An unsupervised-learning-based approach for automated defect inspection on textured surfaces, IEEE Trans. Instrum. *Meas*. 67 (2018) 1266–1277. https://doi.org/10.1109/TIM.2018.2795178.

73. F. Bañon, S. Martin, J.M. Vazquez-Martinez, J. Salguero, F.J. Trujillo, Predictive models based on RSM and ANN for roughness and wettability achieved by laser texturing of S275 carbon steel alloy, *Opt Laser Technol*. 168 (2024) 109963. https://doi.org/10.1016/j.optlastec.2023.109963.

74. T. Steege, G. Bernard, P. Darm, T. Kunze, A.F. Lasagni, Prediction of Surface Roughness in Functional Laser Surface Texturing Utilizing Machine Learning, *Photonics*. 10 (2023) 361. https://doi.org/10.3390/photonics10040361.

75. L. Moles, I. Llavori, A. Aginagalde, G. Echegaray, D. Bruneel, F. Boto, A. Zabala, On the use of machine learning for predicting femtosecond laser grooves in tribological applications, *Tribol Int.* 200 (2024) 110067. https://doi.org/10.1016/j.triboint.2024.110067.

76. M.D.T. McDonnell, D. Arnaldo, E. Pelletier, J.A. Grant-Jacob, M. Praeger, D. Karnakis, R.W. Eason, B. Mills, Machine learning for multi-dimensional optimisation and predictive visualisation of laser machining, *J Intell Manuf.* 32 (2021) 1471–1483. https://doi.org/10.1007/s10845-020-01717-4.

Copyright © by DILAPRO All Rights Reserved